STAR Heavy Ion Update

Xin Dong (Lawrence Berkeley National Laboratory)
for the STAR Collaboration

- HI Run Status and Publication Records
- Recent Highlights
  - CME, Initial Geometry and EM Field (isobar, AuAu)
  - Hot QCD Medium Properties (isobar, AuAu)
  - QCD Phase Structure at High μ_B (BES-I/II + FXT)

STAR Run21

Single-Beam Energy (GeV/nucleon)	$\sqrt{s_{NN}}$ (GeV)	Run Time	Species	Events (MinBias)	Priority	Date Completed In 2021
3.85	7.7	11-20 weeks	Au+Au	100 M	1	← May 1
3.85	3 (FXT)	3 days	Au+Au	300 M	2	← May 5
44.5	9.2 (FXT)	0.5 days	Au+Au	50 M	2	← May 6
70	11.5 (FXT)	0.5 days	Au+Au	50 M	2	← May 7
100	13.7 (FXT)	0.5 days	Au+Au	50 M	2	← May 8
100	200	1 week	O+O	400 M 200 M (central)	3	← May 24
8.35	17.1	2.5 weeks	Au+Au	250 M	3	← June 7
3.85	3 (FXT)	3 weeks	Au+Au	2 B	3	← June 28
100	200	1 week	d+Au	100M (MB) / 100M (0-10%)		← July 7

Additional d+Au @ 200 GeV data recorded with EPD (2.2<|η|<5.2) and iTPC (|η|<1.5)

- expect a reduction of statistical uncertainty by x8 for 2-particle correlation method

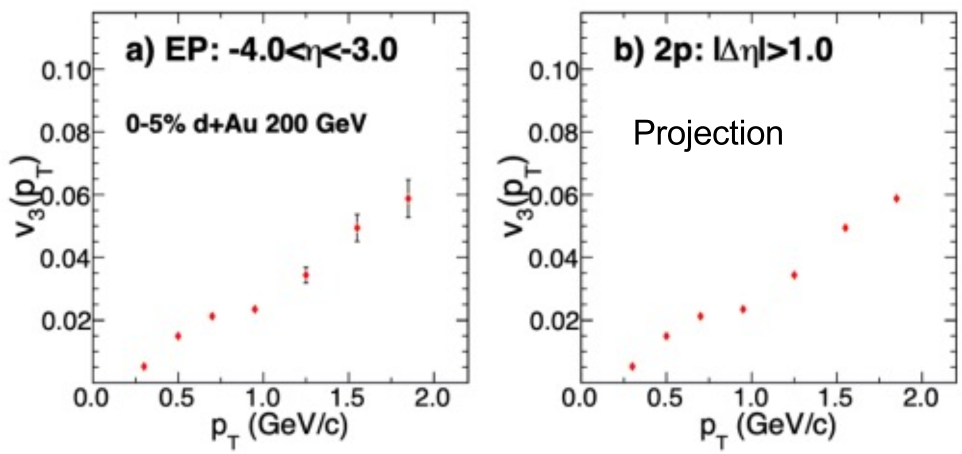

Publication Record

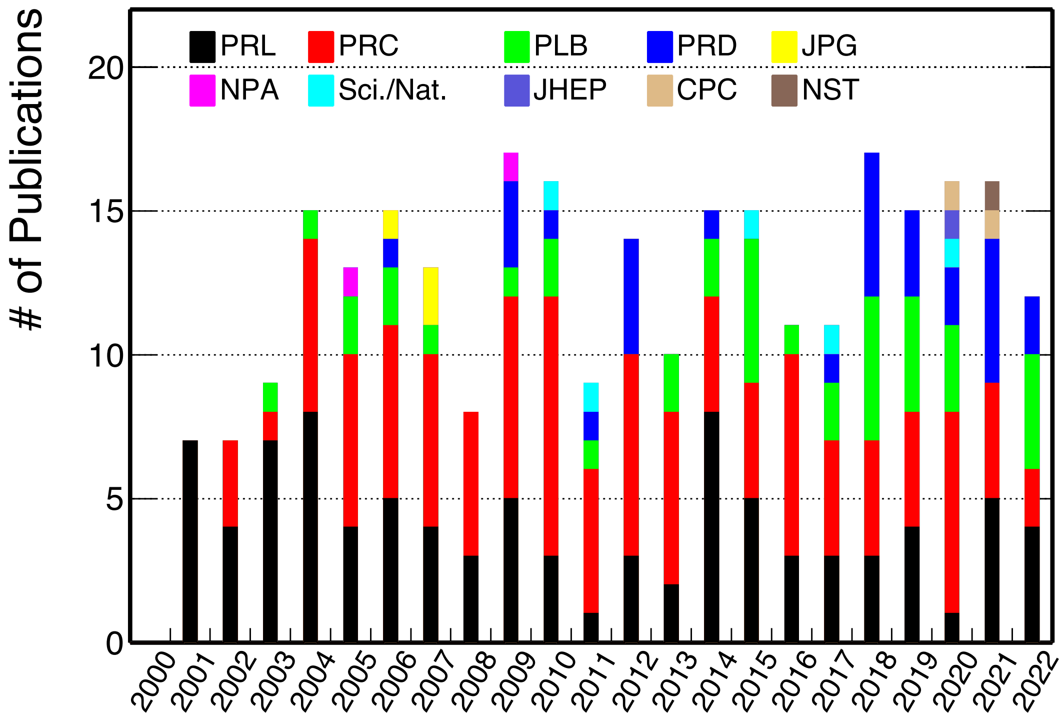

16 publications (5 PRLs) in 2021

12 publications (4 PRLs) in 2022

11 papers under journal review

28 active GPCs

Quark Matter 2022 conference (April, 2022, Krakow, Poland):
22 parallel talks, 47 posters, 2 flash talks

Strangeness in Quark Matter 2022 conference (June, 2022, Busan, Korea):
15 parallel talks

Published and Submitted Papers After PAC 2021

ColdQCD

1. Azimuthal transverse single-spin asymmetries of inclusive jets and identified hadrons within jets from polarized pp collisions at sqrt{s} = 200 GeV *Submitted* arXiv:2205.11800
2. Evidence for Nonlinear Gluon Effects in QCD and their A Dependence at STAR *Submitted* arXiv:2111.10396
3. Longitudinal double-spin asymmetry for inclusive jet and dijet production in polarized proton collisions at $\sqrt{s}=510$ GeV Phys. Rev. D 105 (2022) 92011

JetCorr

4. Two-particle correlations on transverse rapidity in Au+Au collisions at sqrt{sNN} = 200 GeV at STAR *Submitted* arXiv:2204.11661
5. PYTHIA8 underlying event tune for RHIC energies Phys. Rev. D 105 (2022) 16011
6. Differential measurements of jet substructure and partonic energy loss in Au+Au collisions at sqrt(s_NN) =200 GeV Phys. Rev. C 105 (2022) 44906
7. Invariant jet mass measurements in pp collisions at sqrt(s) = 200 GeV at RHIC Phys. Rev. D 104 (2021) 52007

Heavy Flavor

8. Evidence of Mass Ordering of Charm and Bottom Quark Energy Loss in Au+Au Collisions at RHIC *Submitted* arXiv:2111.14615
9. Measurement of cold nuclear matter effects for inclusive J/psi in p+Au collisions at sqrt(sNN) = 200 GeV Phys. Lett. B 825 (2022) 136865
10. Measurement of inclusive electrons from open heavy-flavor hadron decays in p+p collisions at $\sqrt{s} = 200$ GeV with the STAR detector Phys. Rev. D 105 (2022) 32007
11. Observation of Ds/D0 Enhancement in Au+Au Collisions at sqrt(s_NN) = 200 GeV Phys. Rev. Lett. 127 (2021)

LFSUPC

12. **Probing Strangeness Canonical Ensemble with K-, phi(1020) and Xi- Production in Au+Au Collisions at sqrt{s_NN} = 3 GeV Accepted arXiv:2108.00924**
13. **Measurements of H3L and H4L Lifetimes and Yields in Au+Au Collisions in the High Baryon Density Region Phys. Rev. Lett. 128 (2022) 202301**
14. Tomography of Ultra-relativistic Nuclei with Polarized Photon-gluon Collisions *Submitted* arXiv:2204.01625
15. Probing the Gluon Structure of the Deuteron with J/psi Photoproduction in d+Au Ultraperipheral Collisions Phys. Rev. Lett. 128 (2022) 122303
16. Measurement of e+e- Momentum and Angular Distributions from Linearly Polarized Photon Collisions Phys. Rev. Lett. 127 (2021) 52302

Correlation & Fluctuation

17. Measurements of Proton High Order Cumulants in sqrt{s_NN} = 3 GeV Au+Au Collisions and Implications for the QCD Critical Point Phys. Rev. Lett. 128 (2022) 202303
18. Measurement of the Sixth-Order Cumulant of Net-Proton Multiplicity Distributions in Au+Au Collisions at sqrt{sNN} = 27 , 54.4, and 200 GeV at RHIC Phys. Rev. Lett. 127 (2021) 262301
19. Cumulants and correlation functions of net-proton, proton, and antiproton multiplicity distributions in Au+Au collisions at energies available at the BNL Relativistic Heavy Ion Collider Phys. Rev. C 104 (2021) 24902

Flow, Chirality and Vorticity

20. Azimuthal anisotropy measurement of (multi-)strange hadrons in Au+Au collisions at sqrt(s_NN) = 54.4 GeV *Submitted* arXiv:2205.11073
21. Observation of Global Spin Alignment of phi and K*0 Vector Mesons in Nuclear Collisions *Submitted* arXiv:2204.02302
22. Centrality and transverse momentum dependence of higher-order flow harmonics of identified hadrons in Au+Au collisions at $\sqrt{s_{\rm NN}}$ = 200 GeV *Submitted* arXiv:2203.07204
23. Pair invariant mass to isolate background in the search for the chiral magnetic effect in Au+Au collisions at sqrt(sNN) = 200 GeV *Submitted* arXiv:2006.05035
24. Collision-system and beam-energy dependence of anisotropic flow fluctuations *Submitted* arXiv:2201.10365
25. **Light Nuclei Collectivity from 3 GeV Au+Au Collisions at RHIC Phys. Lett. B 827 (2022) 136941**
26. **Disappearance of partonic collectivity in 3 GeV Au+Au collisions at RHIC Phys. Lett. B 827 (2022) 137003**
27. **Search for the chiral magnetic effect with isobar collisions at sqrt{sNN} = 200 GeV by the STAR Collaboration at the BNL Relativistic Heavy Ion Collider Phys. Rev. C 105 (2022) 14901 - isobar CME blinding analysis**
28. Search for the Chiral Magnetic Effect via Charge-Dependent Azimuthal Correlations Relative to Spectator and Participant Planes in Au+Au Collisions sqrt{s_NN} = 200 GeV Phys. Rev. Lett. 128 (2022) 92301
29. **Global Lambda-hyperon polarization in Au+Au collisions at sqrt{sNN} =3 GeV Phys. Rev. C 104 (2021) 61901**
30. Investigation of Experimental Observables in Search of the Chiral Magnetic Effect in Heavy-ion Collisions in the STAR experiment Chinese Phys. C 46 (2022) 14101

Blinding Analysis of CME Search with Isobar Data

Mock data challenge
Test data structure
(27 GeV files)

Isobar-Mixed Analysis
QA, physics & code freezing
(One run is Ru+Zr)

Isobar-Blind Analysis
Run-by-run QA, full analysis
(One run is Ru/Zr)

Isobar-Unblind Analysis
Full analysis
(Ru and Zr separated)

→ Publication of Blind Analysis

CPC 46 (2022) 14101

Pre-defined signature of CME: $$\frac{\langle \mathrm{Observable} \rangle_{\mathrm{Ru+Ru}}}{\langle \mathrm{Observable} \rangle_{\mathrm{Zr+Zr}}} > 1$$

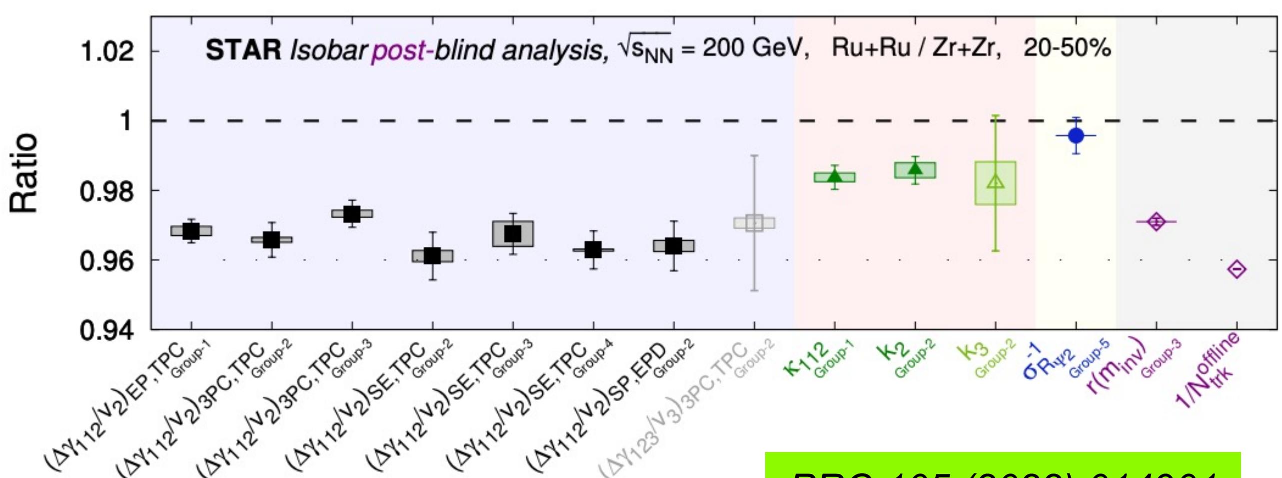

Precision of 0.4% achieved

No pre-defined signature of CME is observed

- possible residual signal due to change of baseline & non-flow effects are under study

PRC 105 (2022) 014901

Blinding Analysis of CME Search with Isobar Data

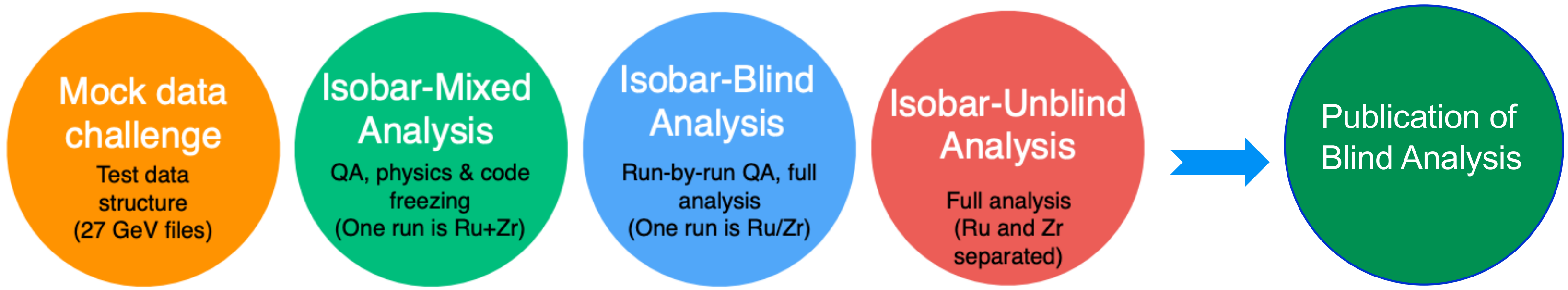

STAR, PRC 105 (2022) 014901

Pre-defined signature of CME: $\frac{\langle\text{Observable}\rangle_{\text{Ru+Ru}}}{\langle\text{Observable}\rangle_{\text{Zr+Zr}}} > 1$

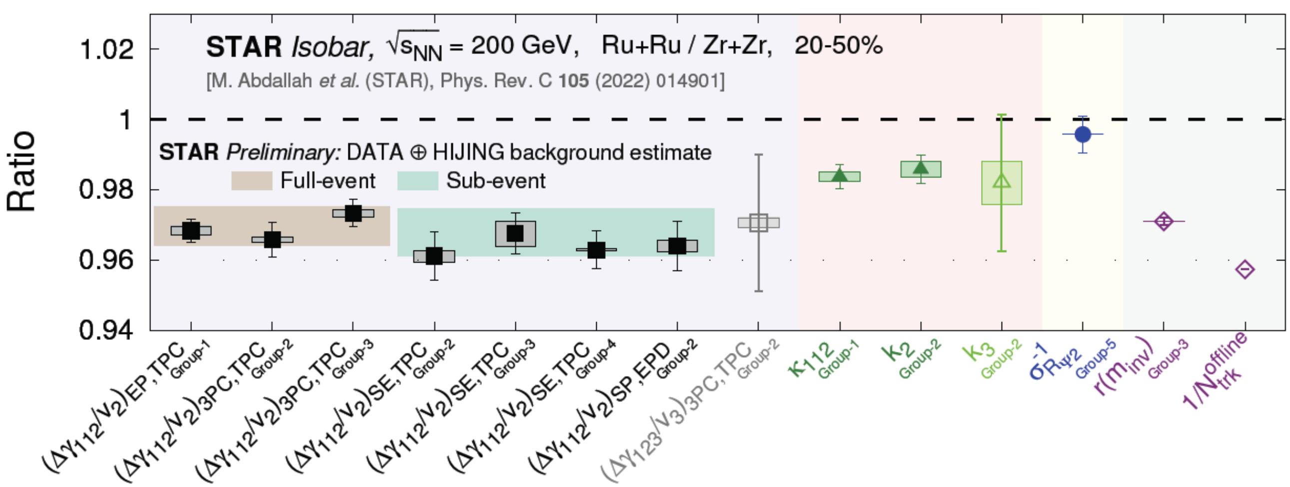

Updated estimate on non-flow combining data/HIJING consistent with isobar data of $\Delta\gamma/v_2$

Hints of signals in Au+Au 200GeV:
PRL 128 (2022) 092301
arXiv: 2006.05035

Nuclear Deformation and Neutron Skin

STAR

v_2 and v_3 in central collisions
→ nuclear deformation parameters

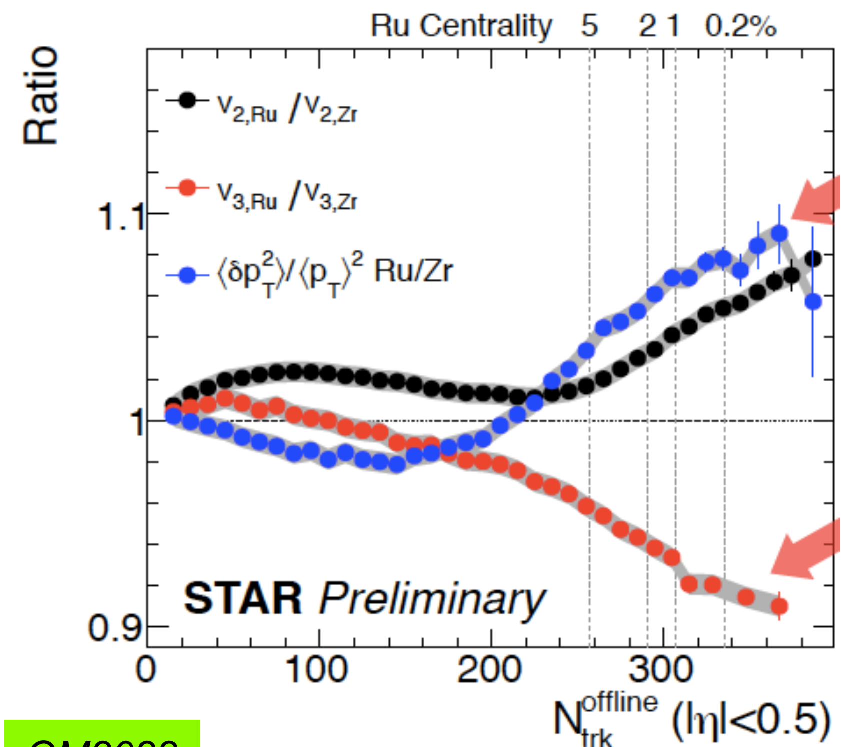

QM2022

β_2(Ru) > β_2(Zr)
β_3(Ru) < β_3(Zr)

Probe neutron skin and symmetry energy

$\Delta r_{np}^{Zr} \gg \Delta r_{np}^{Ru}$ $\quad$ $L(\rho_c) = 3\rho_c \left[\frac{dE_{sym}(\rho)}{d\rho} \right]_{\rho=\rho_c}$

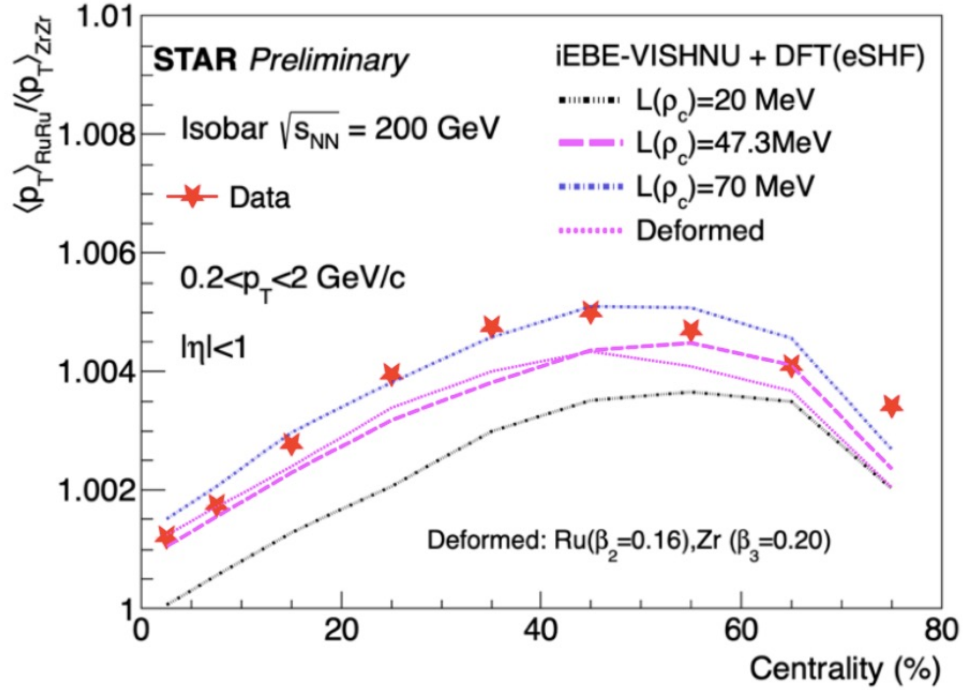

$L(\rho_c)$ = 54 ± 8 MeV from multiplicity ratio
$L(\rho_c)$ = 57 ± 10 MeV from $\langle p_T \rangle$ ratio

Charge and Mass Radius of Nuclei

$$\rho_A(r;R,a) = \frac{\rho_0}{1+\exp[(r-R)/a]},$$

Photo-induced ee and $\rho\to\pi\pi$ production
→ Novel approach to nuclei geometry parameters

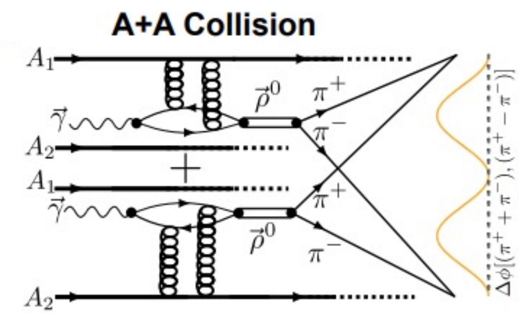

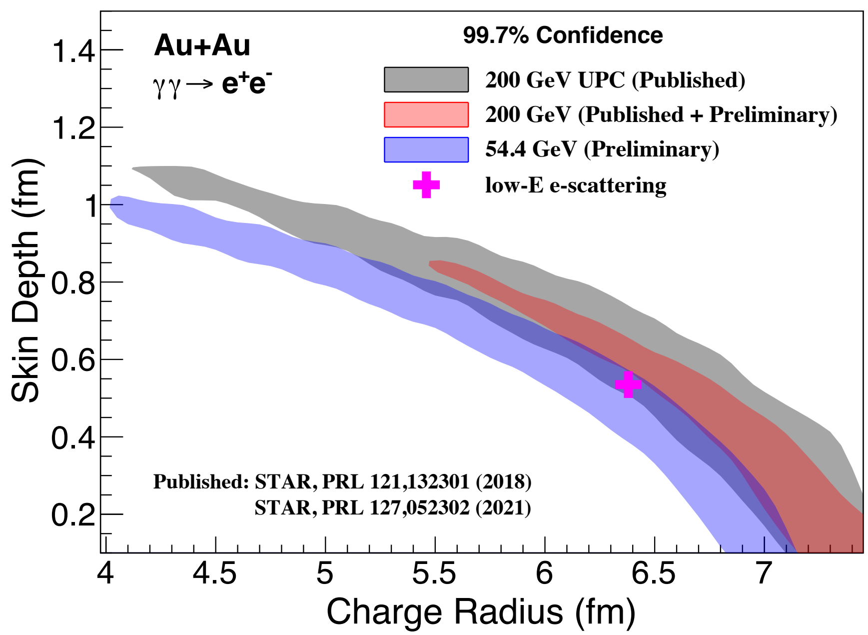

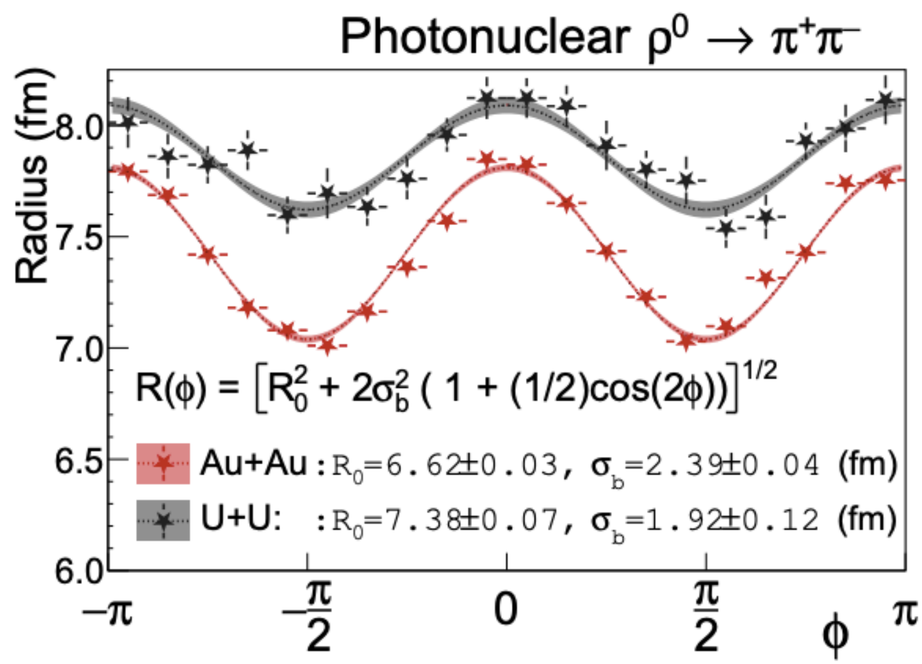

QM2022, 2204.01625

Initial Electromagnetic (EM) Field

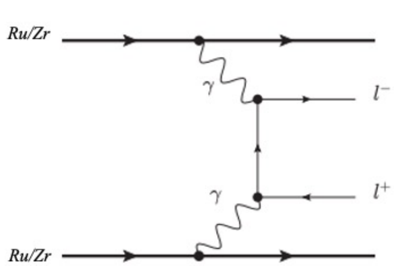

Low p_T dileptons

$$\sigma(\gamma\gamma \to ee) \sim Z^4$$

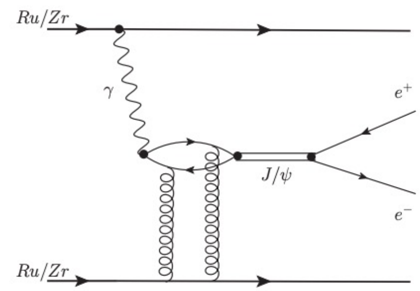

Low p_T J/ψ

$$\sigma(\gamma A \to J/\psi) \sim Z^2$$

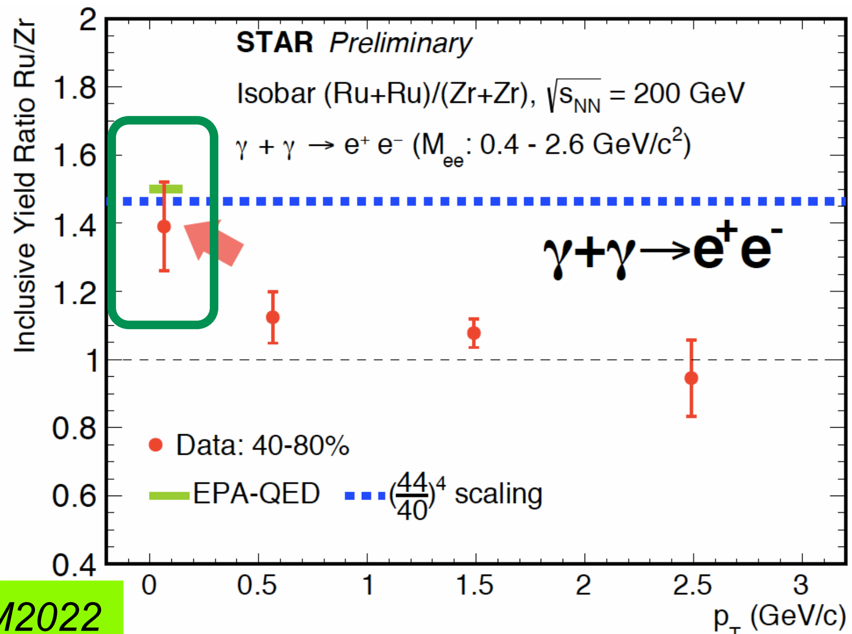

QM2022

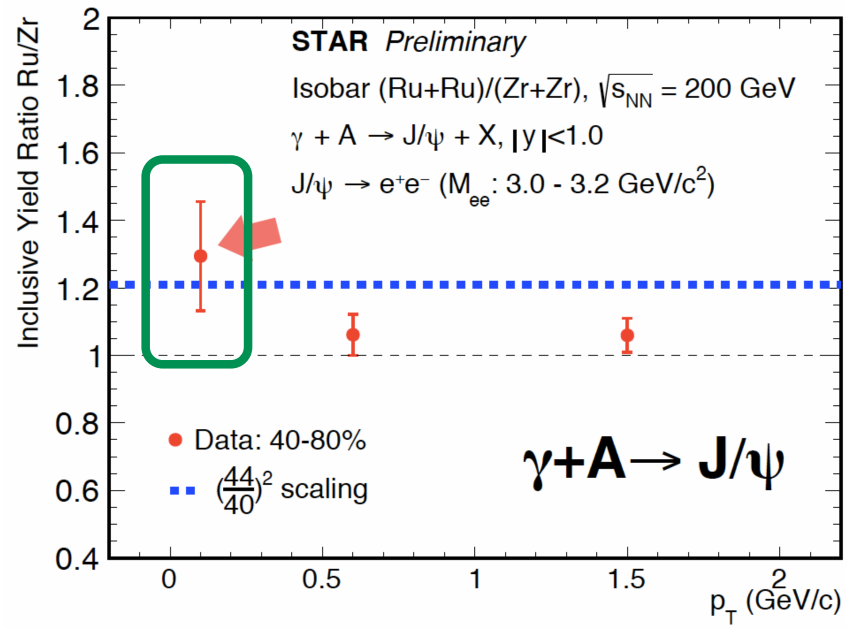

Low p_T dilepton and J/ψ data follow Z-scaling: EM field induced photoproduction

Strong EM Field – v_1 splitting

Initial EM-field + v_1 early stage
→ v_1 split between h+ and h-

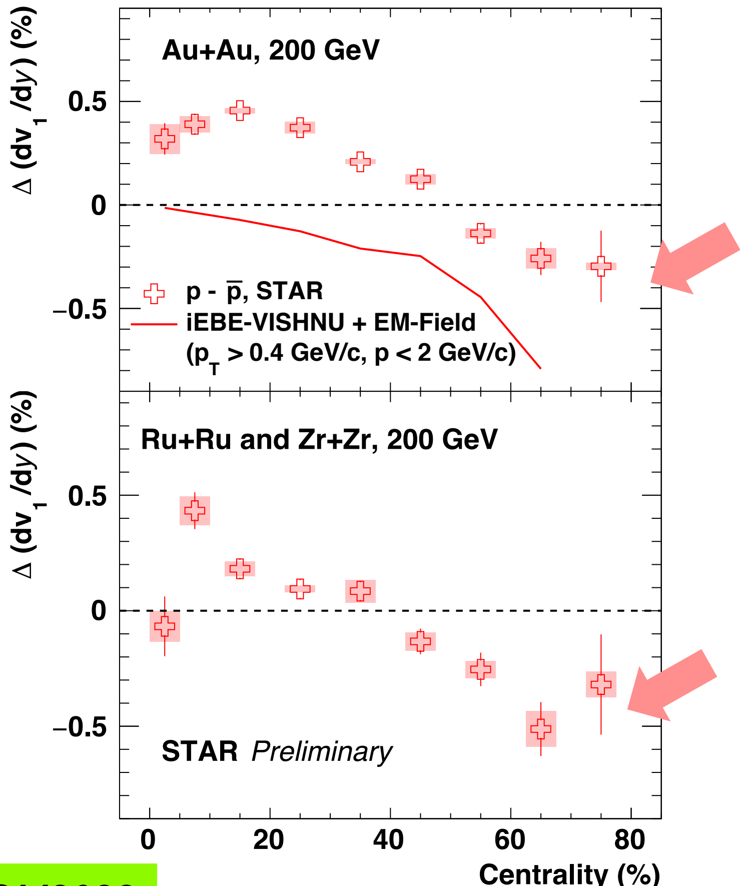

Combination of produced particles
to avoid transport quark effect

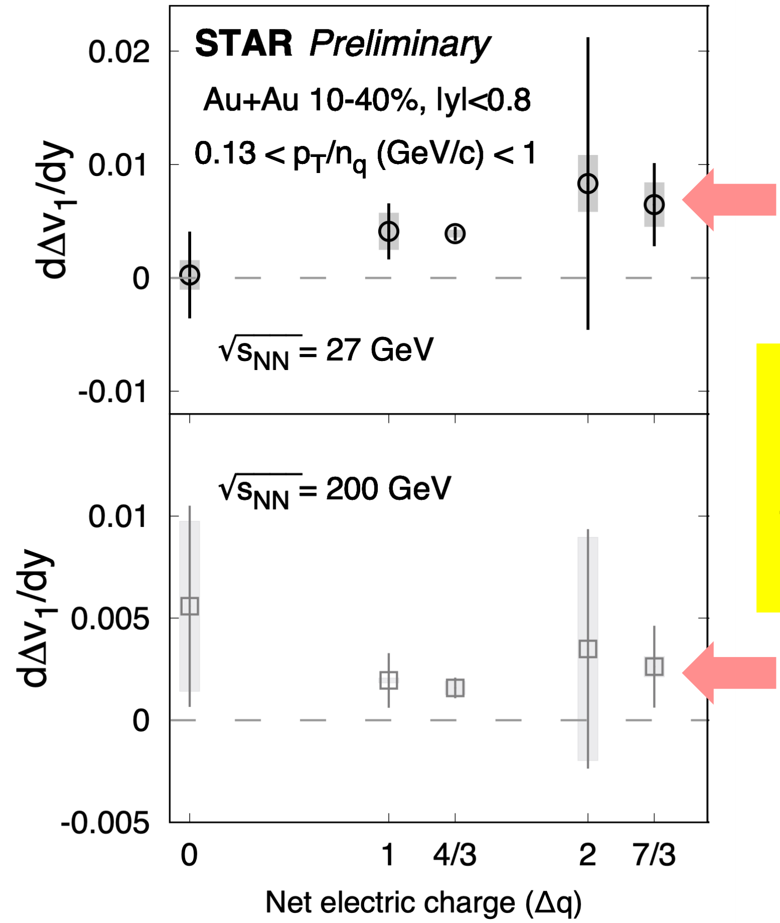

Particle and anti-particle Δv_1
→ evidence for initial EM effect

QM2022

- Hot QCD Medium Properties
  - 3D dynamics
  - Global polarization / spin alignment
  - Gamma-Jets / HF-Jets
  - Medium temperature via dielectrons
  - System size dependence (isobar)

3D Dynamics of Hot QCD Medium

v_n^2–$\langle p_T \rangle$ correlation:

$$\rho(v_n^2, [p_T]) = \frac{\mathrm{cov}(v_n^2, [p_T])}{\sqrt{\mathrm{Var}(v_n^2)}\sqrt{\mathrm{Var}([p_T])}}$$

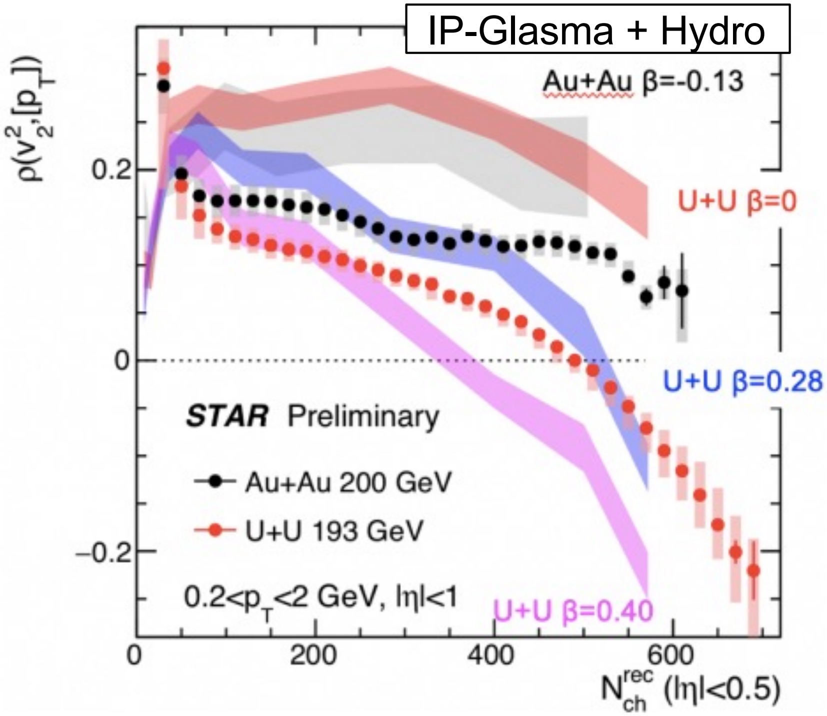

QM2022

Flow decorrelation using BES-II data

$$r_n^v(\eta) = \frac{\langle v_n(-\eta) v_n(\eta_{ref}) \rangle}{\langle v_n(+\eta) v_n(\eta_{ref}) \rangle}$$

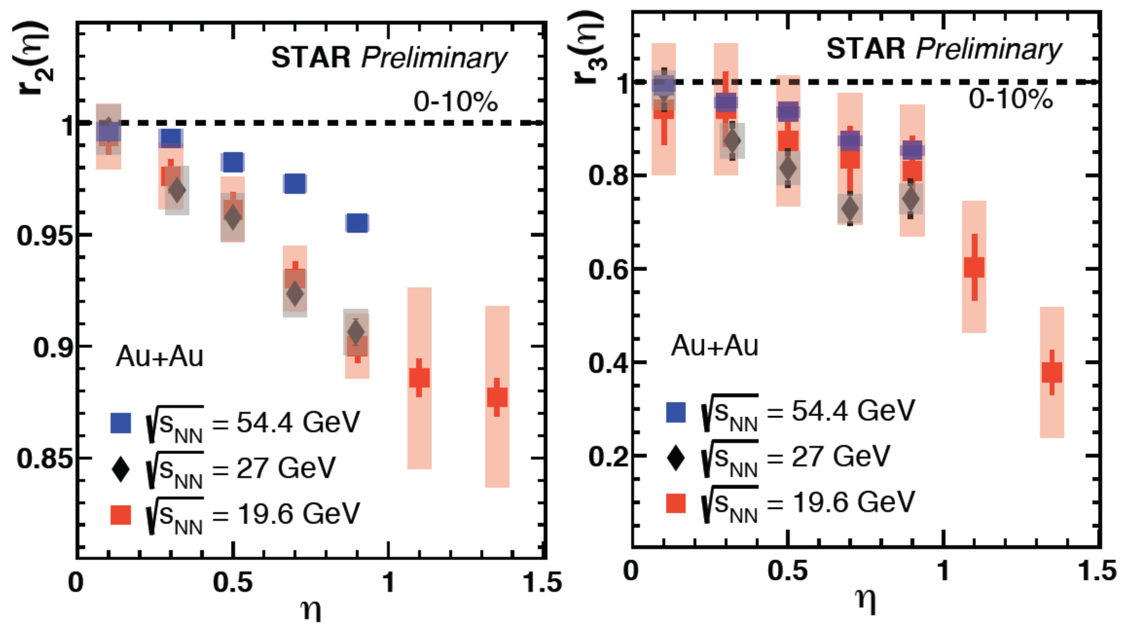

New insights to the 3D dynamics and strong constraints on $\eta/s(T,\mu_B)$ of hot QCD medium

Global Lambda Polarization - Vorticity

- New FXT 3 GeV and BES-II 19.6 GeV results follow a smooth energy dependence trend
- Isobar ~ AuAu in the same centrality bin

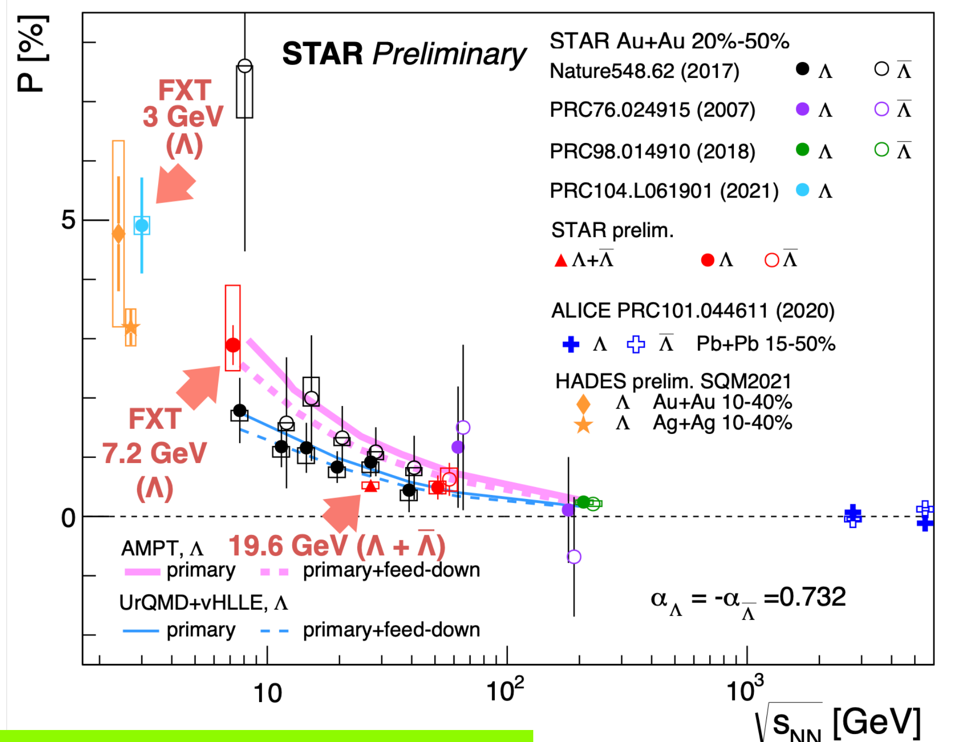

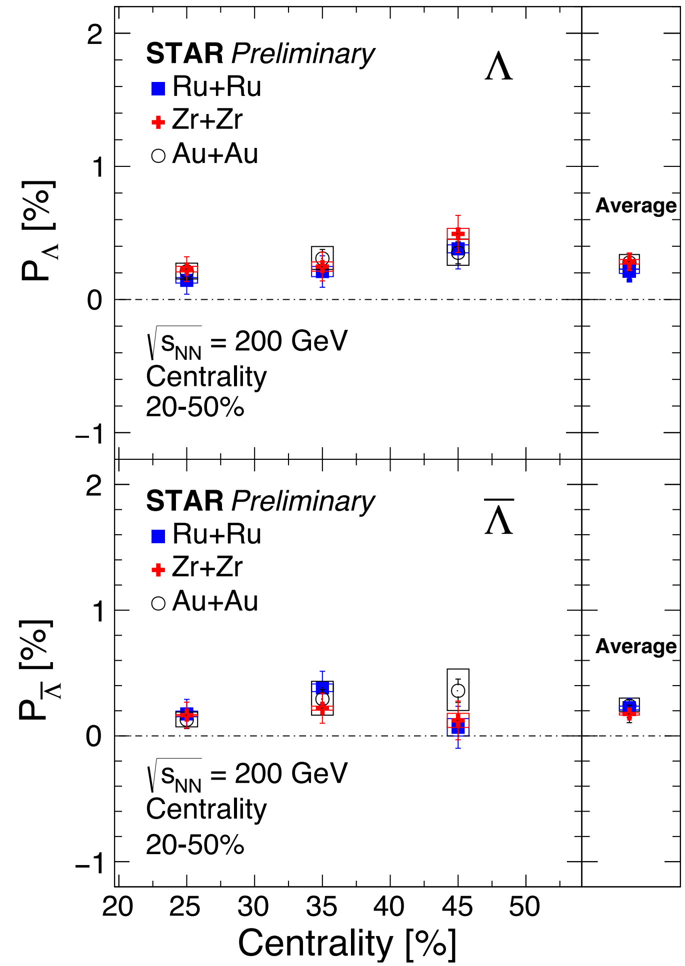

3 GeV: PRC 104 (2021) 061901
7.2 GeV and 19.6 GeV: QM2022

Global Spin Alignment of Vector Mesons

Λ-like (-10^{-5})

Electric field (10^{-5})

$$\rho_{00}(\phi) \approx \frac{1}{3} + c_\Lambda + c_\epsilon + c_E + c_\phi;$$

Vorticity tensor (-10^{-4})

Vector meson field

ϕ–meson ρ_{00} > 1/3 by 8.4σ

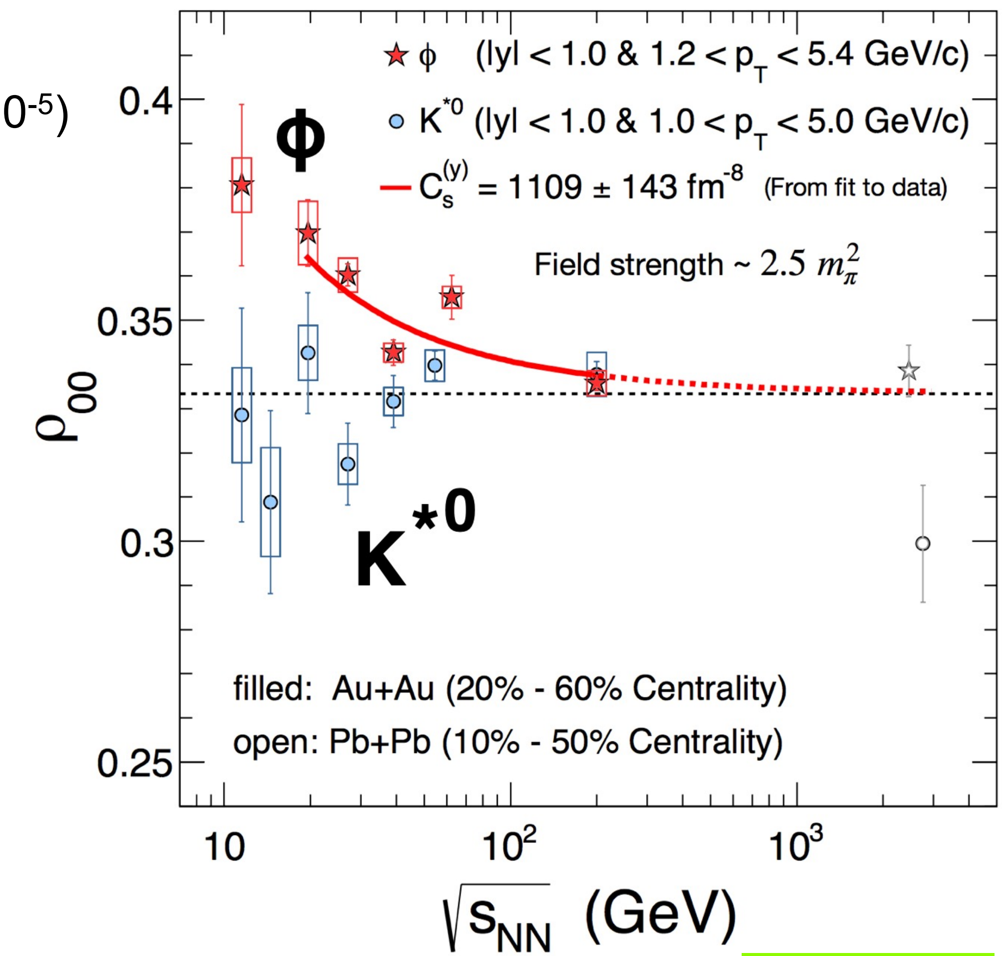

2204.02302

Possible explanation with a strong vector meson field

- p_T/centrality dependence?

Medium-induced Jet Broadening

Semi-inclusive π^0/γ-jets:
Ratio of $R_{0.2}/R_{0.5}$: AuAu < pp
intra-jet broadening

Excess yield at large angle for π^0/γ-jets in AuAu compared pp PYTHIA
medium-induced jet acoplanarity

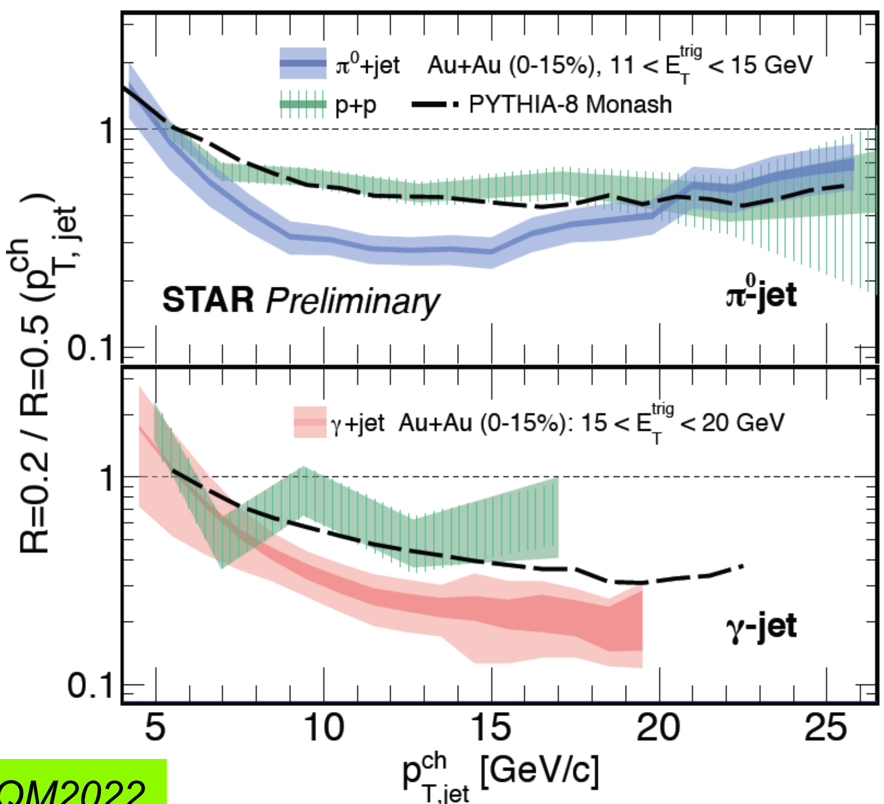

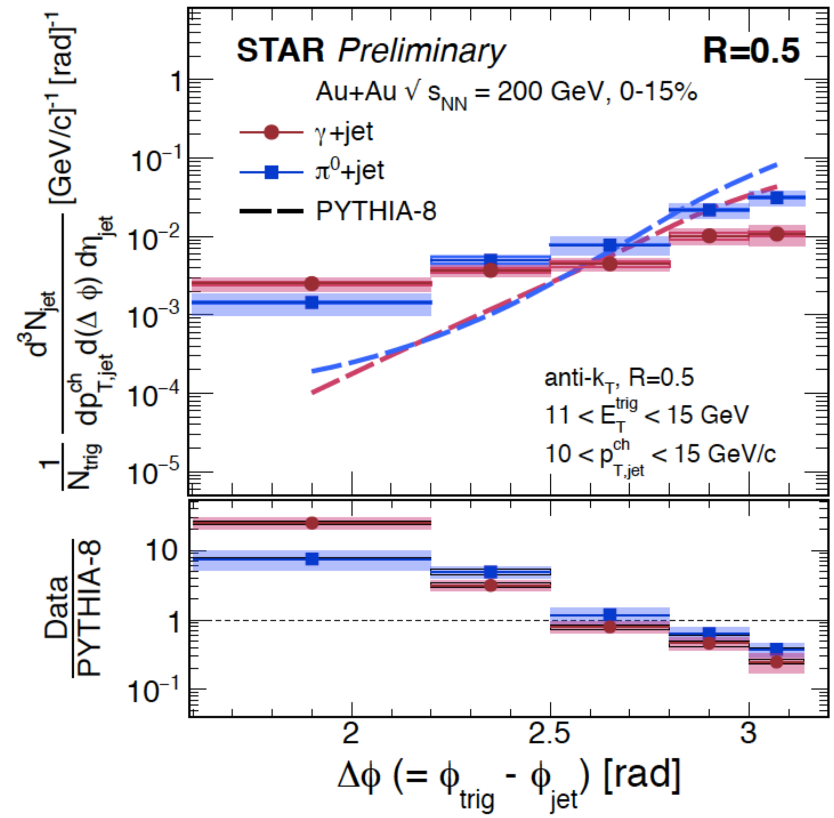

QM2022

Jet Substructure in High-Momentum Di-jet Pairs

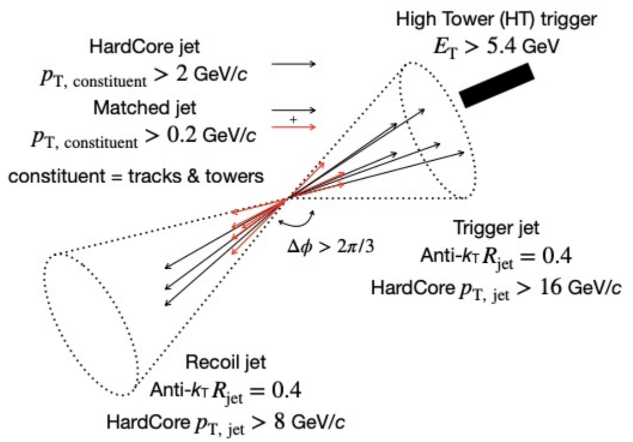

$$A_J \equiv \frac{p_{T,\mathrm{jet}}^{\mathrm{trigger}} - p_{T,\mathrm{jet}}^{\mathrm{recoil}}}{p_{T,\mathrm{jet}}^{\mathrm{trigger}} + p_{T,\mathrm{jet}}^{\mathrm{recoil}}}$$

SoftDrop $z_{\mathrm{cut}} = 0.1,\ \beta = 0$

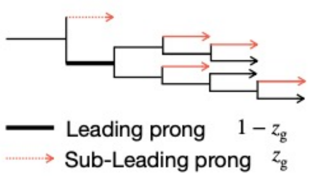

$$z_g = \frac{\min(p_{T,1}, p_{T,2})}{p_{T,1} + p_{T,2}} > z_{\mathrm{cut}} \left(\frac{R_g}{R_{\mathrm{jet}}}\right)^{\beta}$$

$$R_g = \Delta R_{1,2} = \sqrt{\Delta\eta_{1,2}^2 + \Delta\phi_{1,2}^2}$$

Anti-k_T $R_{SJ} = 0.1$ subjets

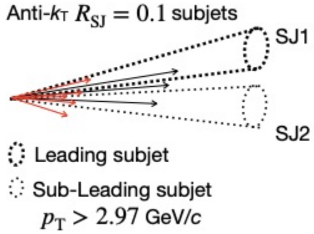

$$z_{SJ} = \frac{\min(p_{T,SJ1}, p_{T,SJ2})}{p_{T,SJ1} + p_{T,SJ2}}$$

$$\theta_{SJ} = \Delta R(\mathrm{SJ1}, \mathrm{SJ2}),$$

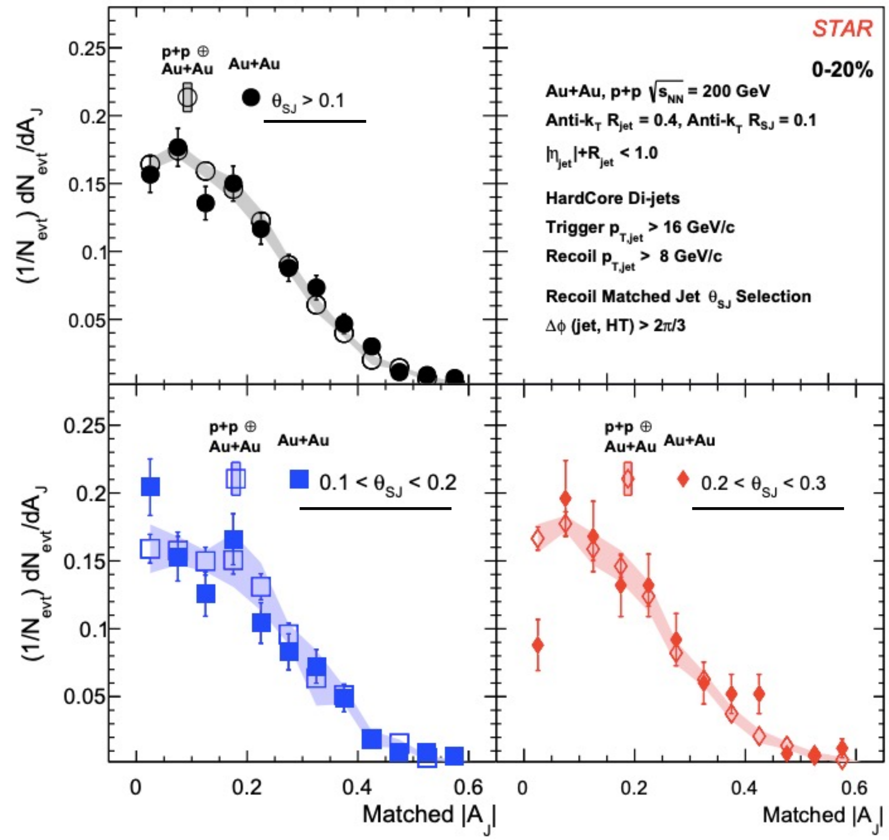

- no significant modifications of groomed observables
- no differences in ΔE signatures in $0.1 < \theta_{SJ} < 0.3$

PRC 105 (2022) 044906

→ ΔE due to gluon radiation from a single color-charge

Dielectrons - Medium Temperature

High statistics di-electron mass spectra from 27 GeV (2018) and 54.4 GeV (2017)
Medium temperature at both low mass (LMR) and intermediate mass (IMR)

T_{IMR} ~ 300 MeV > T_{LMR} ~ 160 MeV ~ T_{pc}

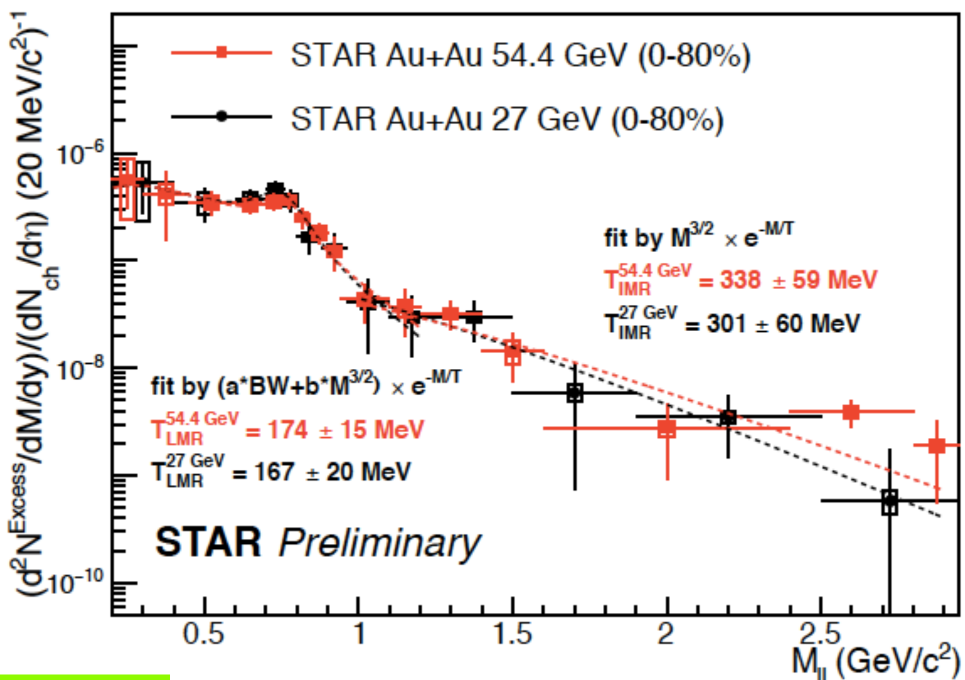

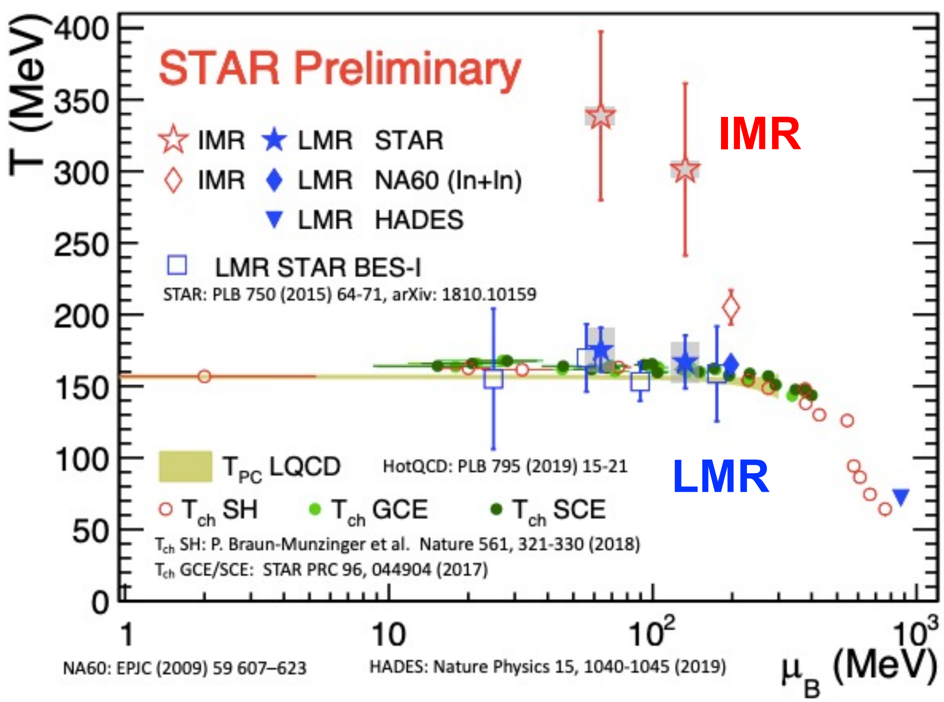

QM2022

Light Hadron and J/ψ from Isobar

High p_T charged hadron and J/ψ suppression scales with N_{part}
- possible bias in peripheral events

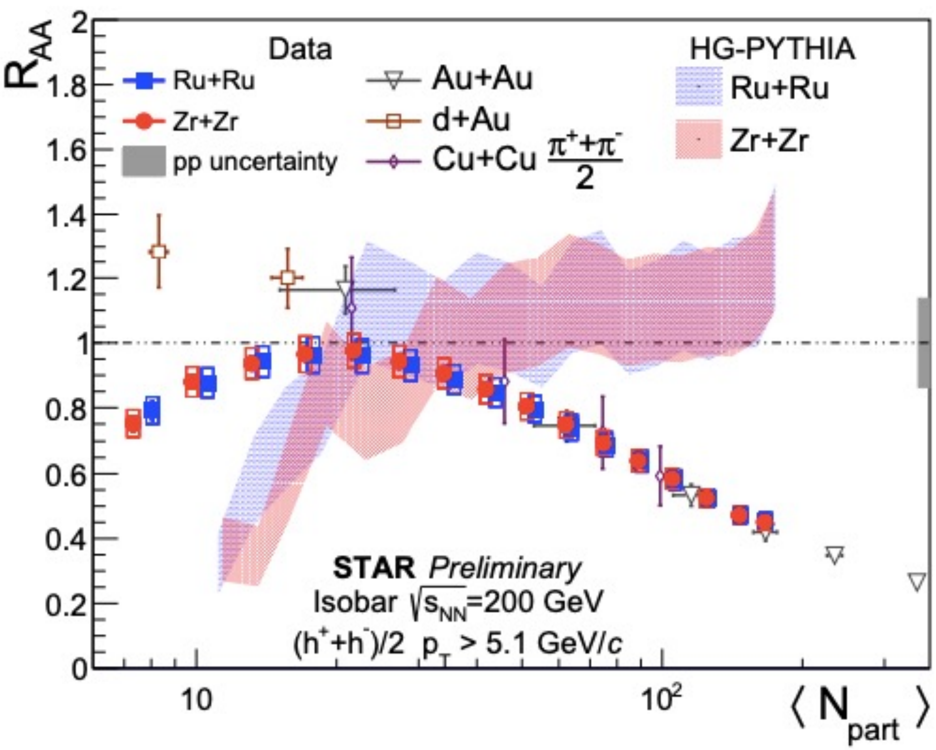

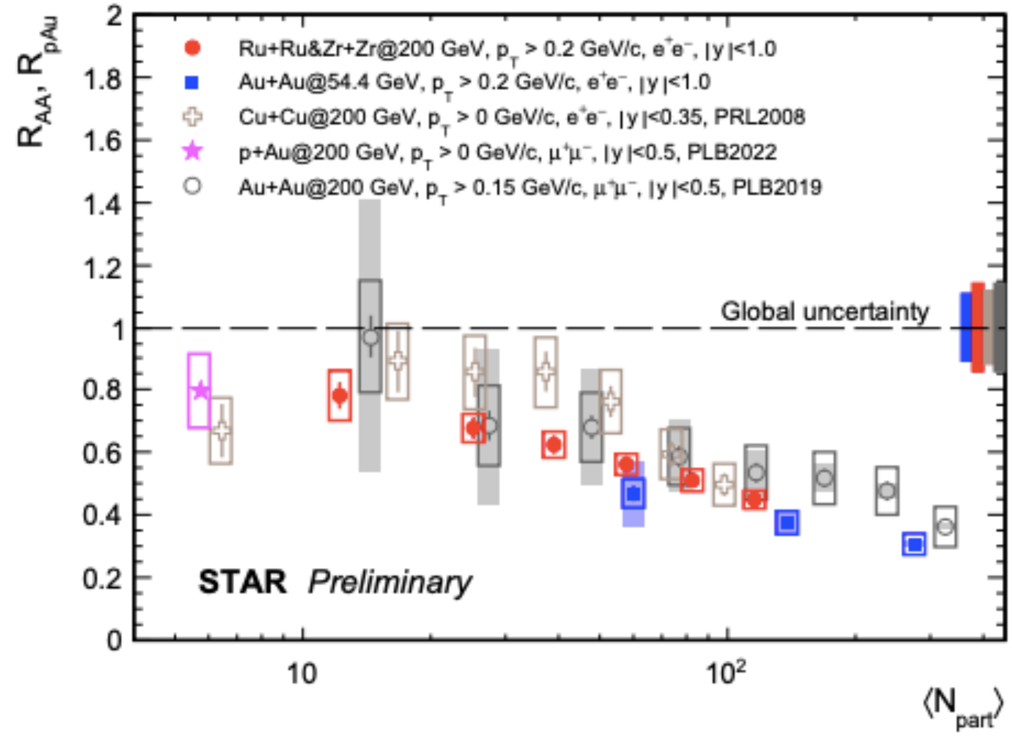

isobar: QM2022 ; pAu: PLB 825 (2022) 136865

Net-proton Cumulants from Isobar

Cumulant ratios (up to C_6) of net-proton from p+p, Au+Au and isobar data

systematic decreasing trend with multiplicity, approaching LQCD calculations (smooth cross over of thermalized medium)

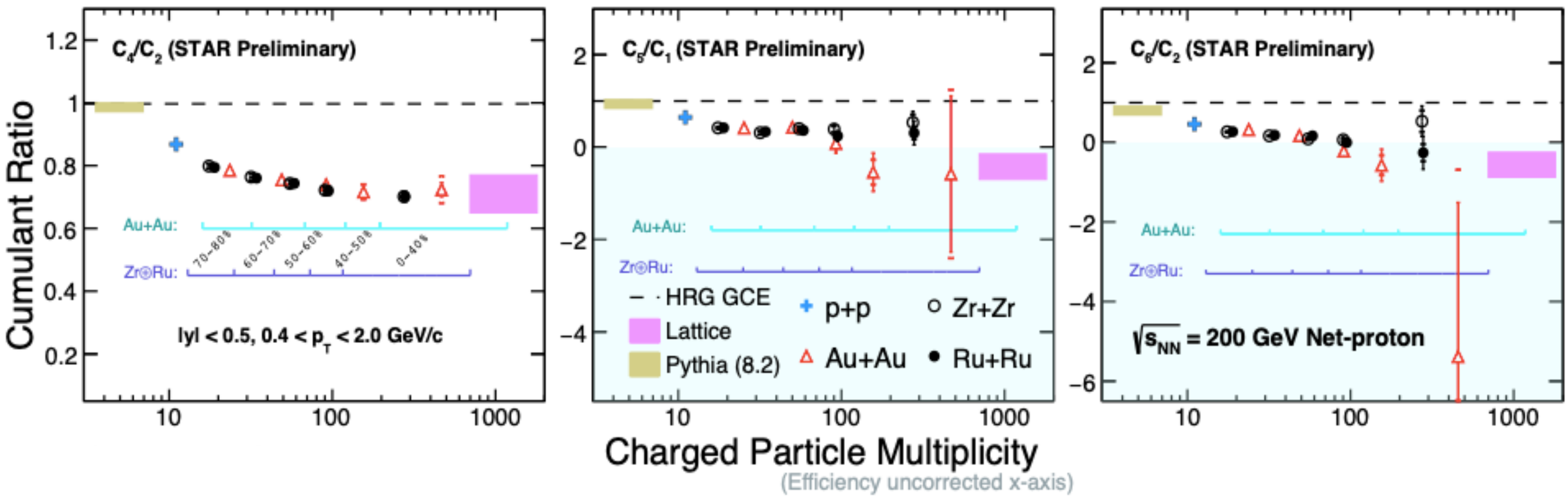

AuAu: PRC 104 (2021) 024902; PRL 127 (2021) 262301
isobar data: QM2022

BES-II Datasets

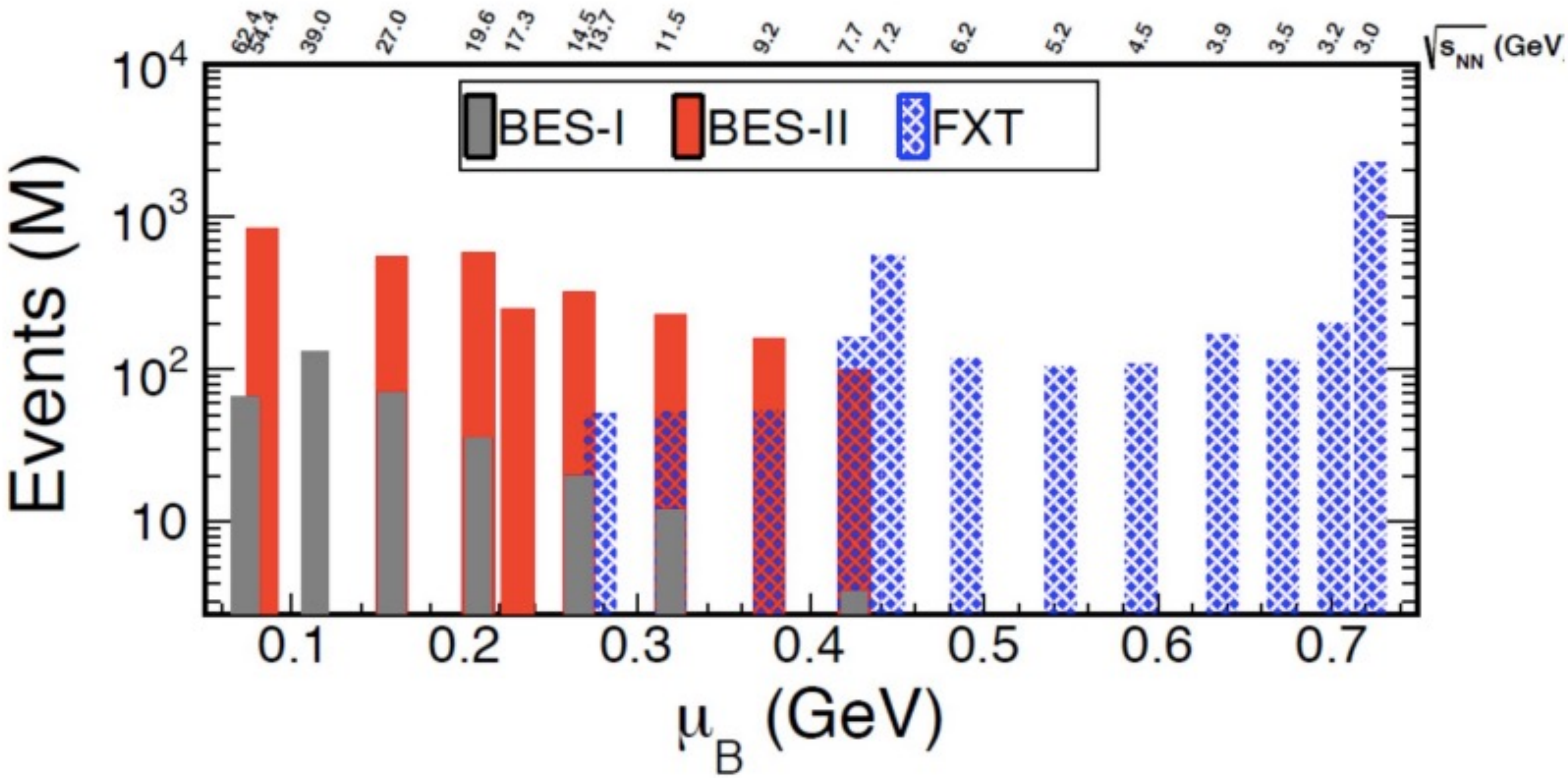

Detector Performance

iTPC (2019+)

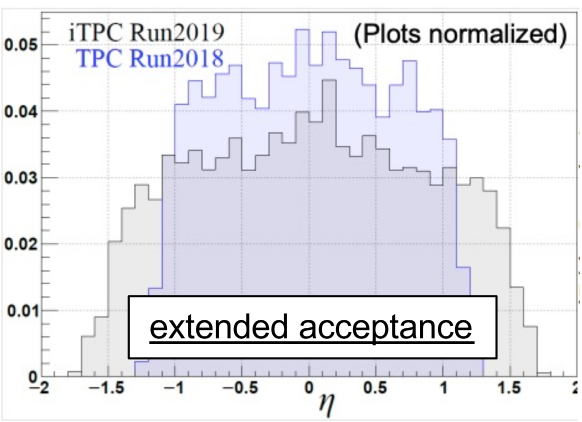

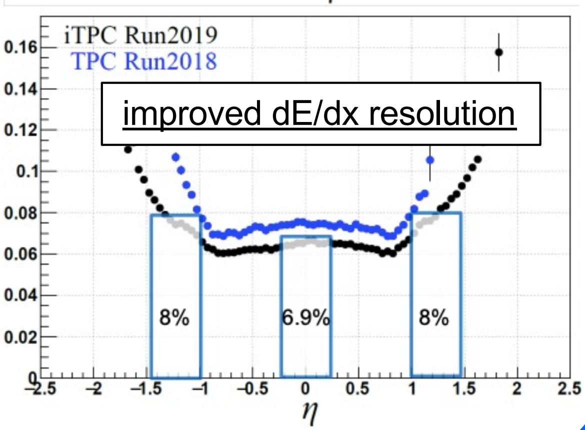

eTOF (2019+)

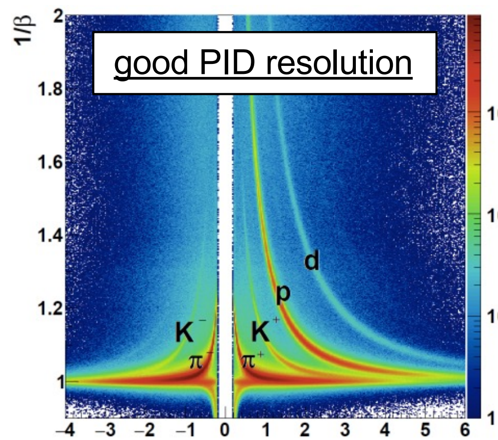

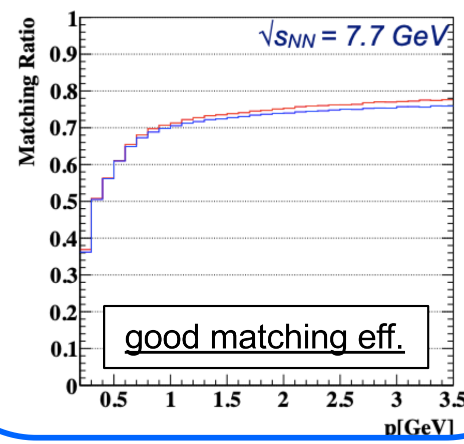

EPD (2018+)

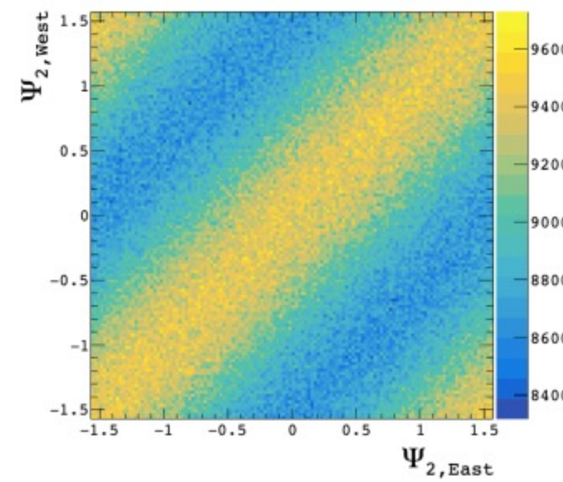

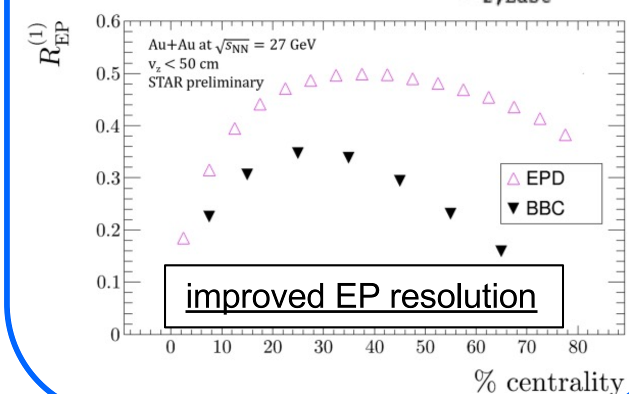

Baryon Stopping

Proton dN/dy from 3 GeV covers mid to target rapidity region
strong centrality dependence in proton rapidity loss

Exponential dependence of proton density with rapidity shift

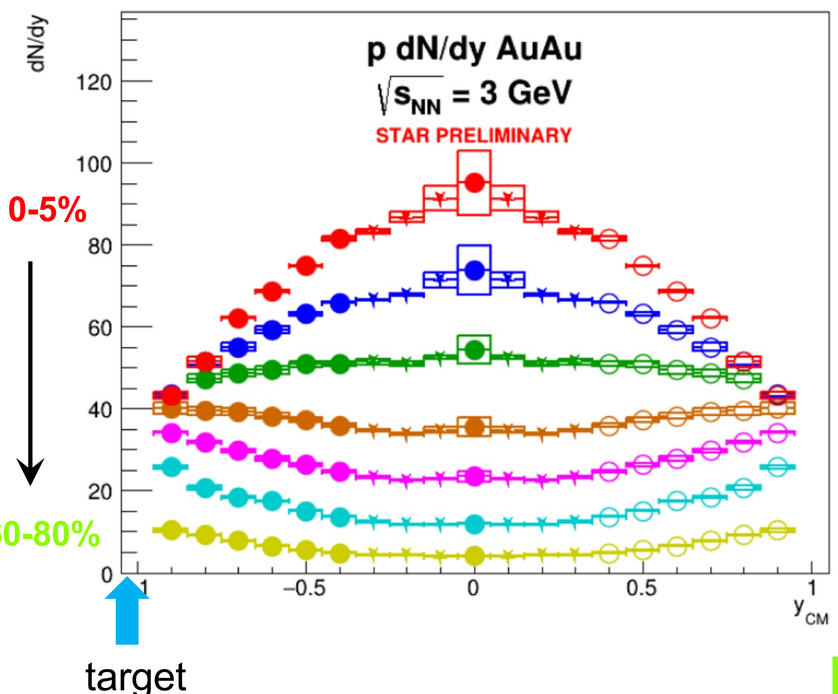

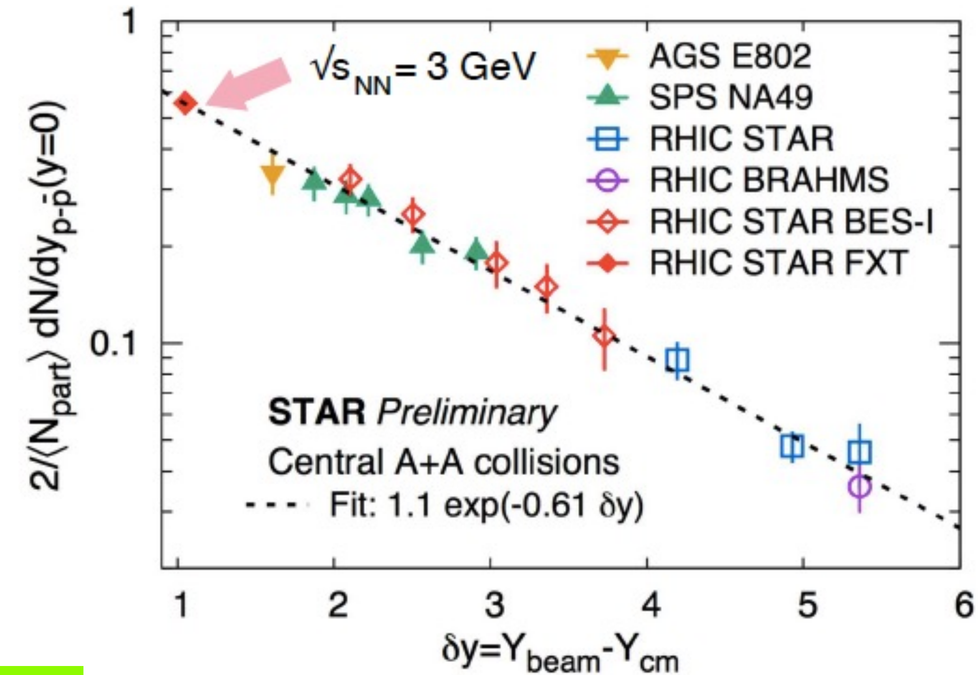

QM2022

Disappearance of Partonic Collectivity at Au+Au 3 GeV

PLB 827 (2022) 137003

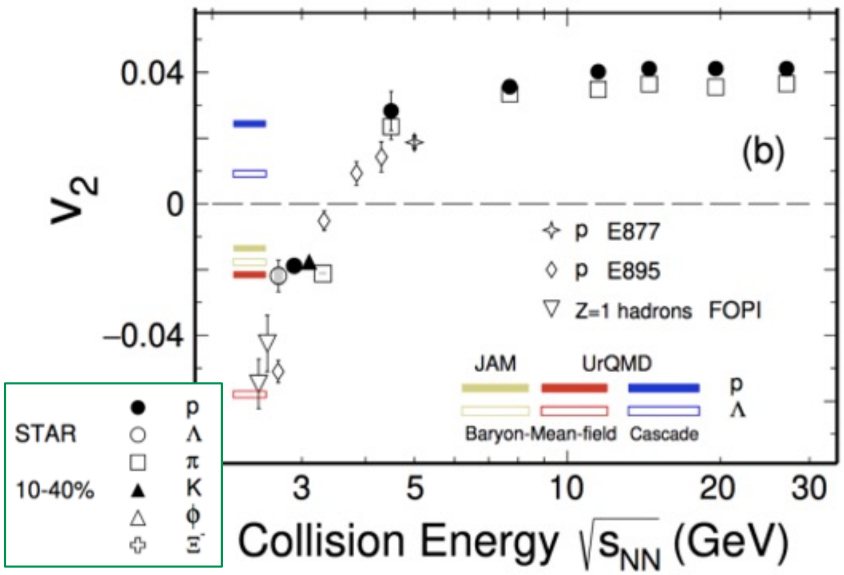

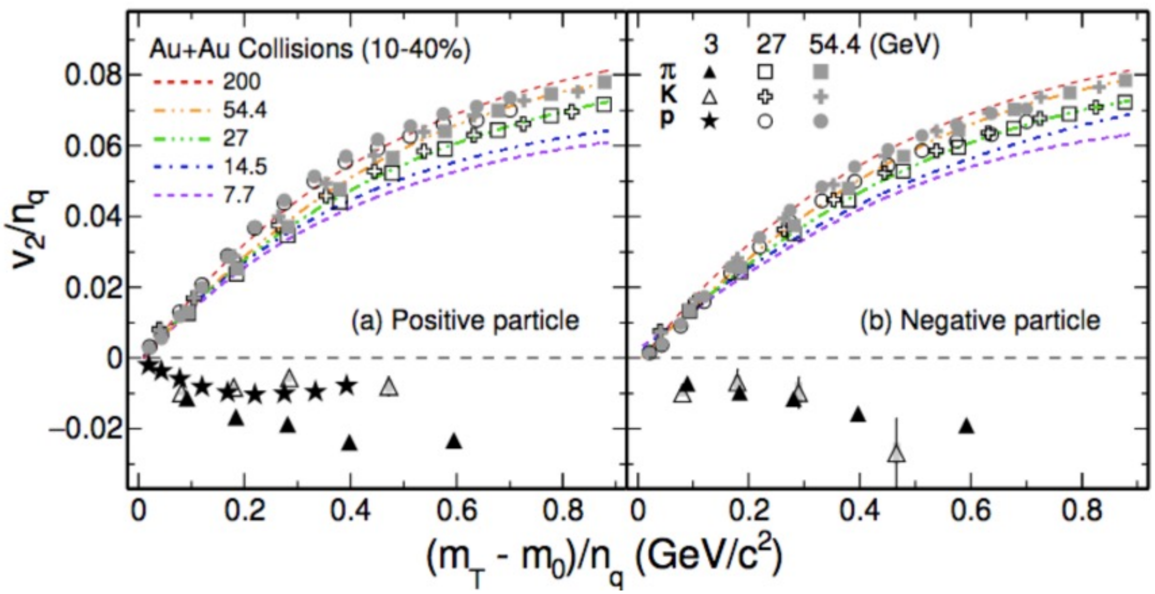

- EPD used for EP determination

Light nuclei collectivity at 3 GeV follows the baryon number scaling – coalescence production

PLB 827 (2022) 136941

- No Number-of-Constituent-Quark scaling at 3 GeV
  - *- UrQMD with baryonic mean-field potential qualitatively consistent with data*

→ Equation-of-State dominated by baryonic interactions in 3 GeV

Multi-strange Hadron Production at 3 GeV

STAR

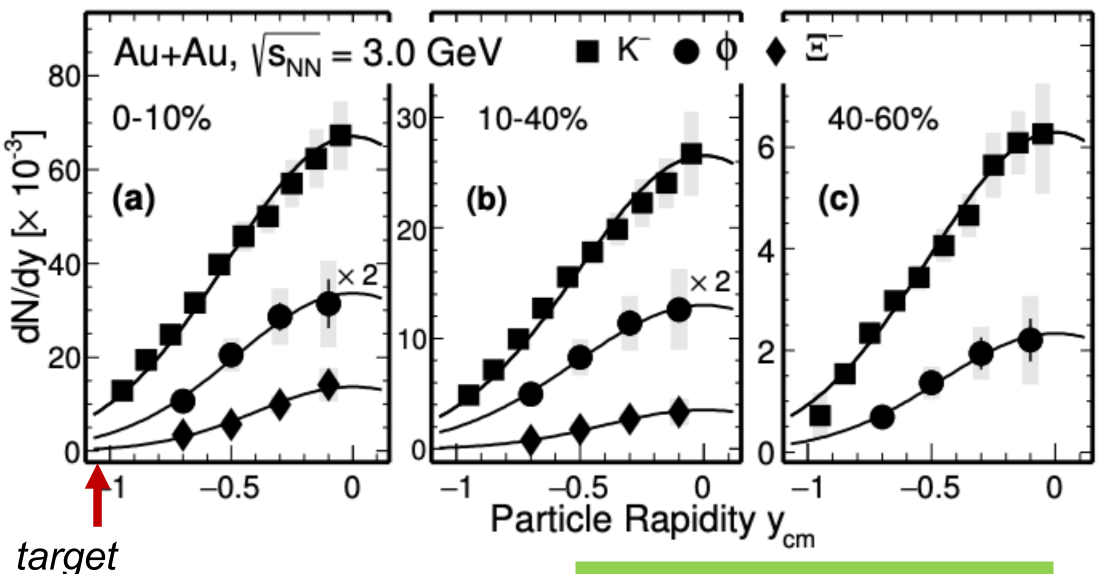

PLB 831 (2022) 137152

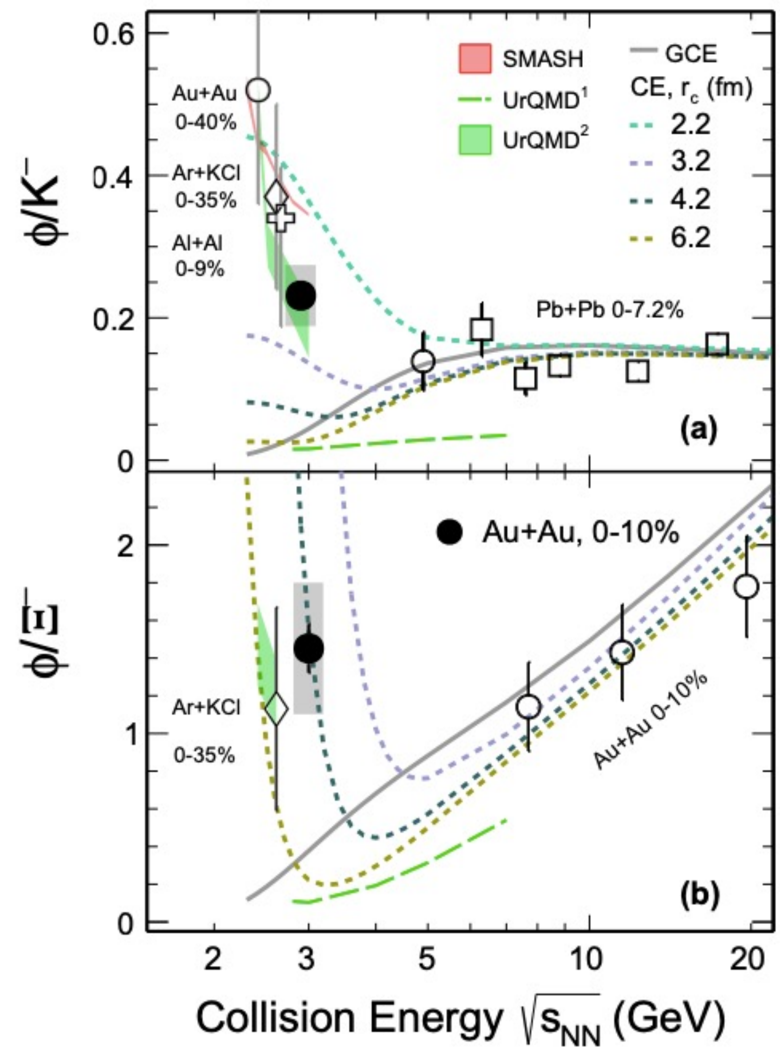

- ϕ/K ratio ~5σ > 0 (~ GCE)
- ϕ/K and ϕ/Ξ favors Canonical Ensemble
  - *favors hadronic models w/ resonance decays*

Hypernuclei Production from BES-II

PRL 128 (2022) 202301, QM2022

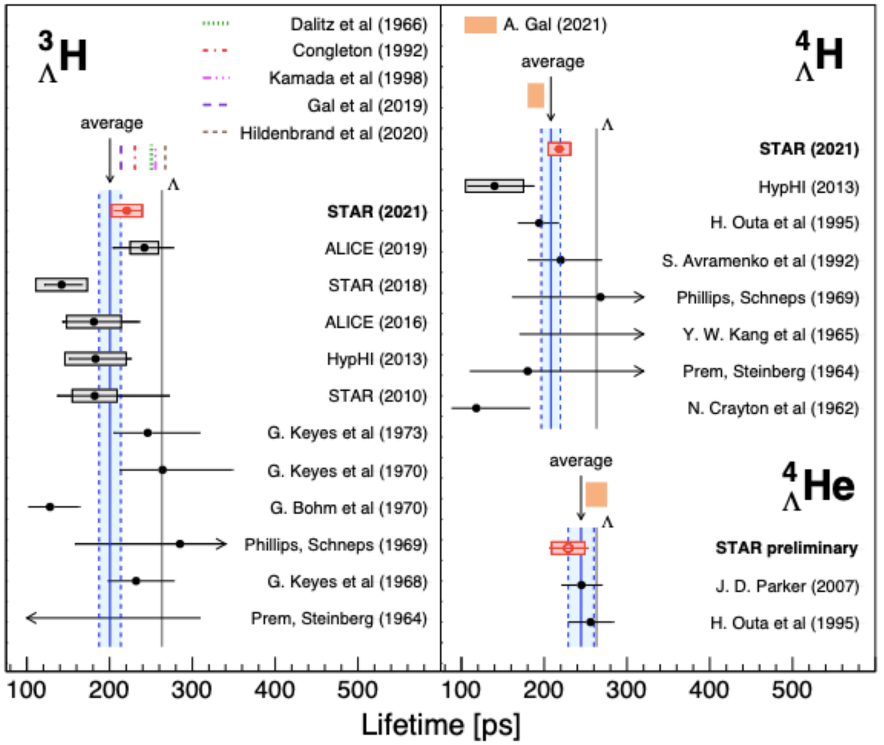

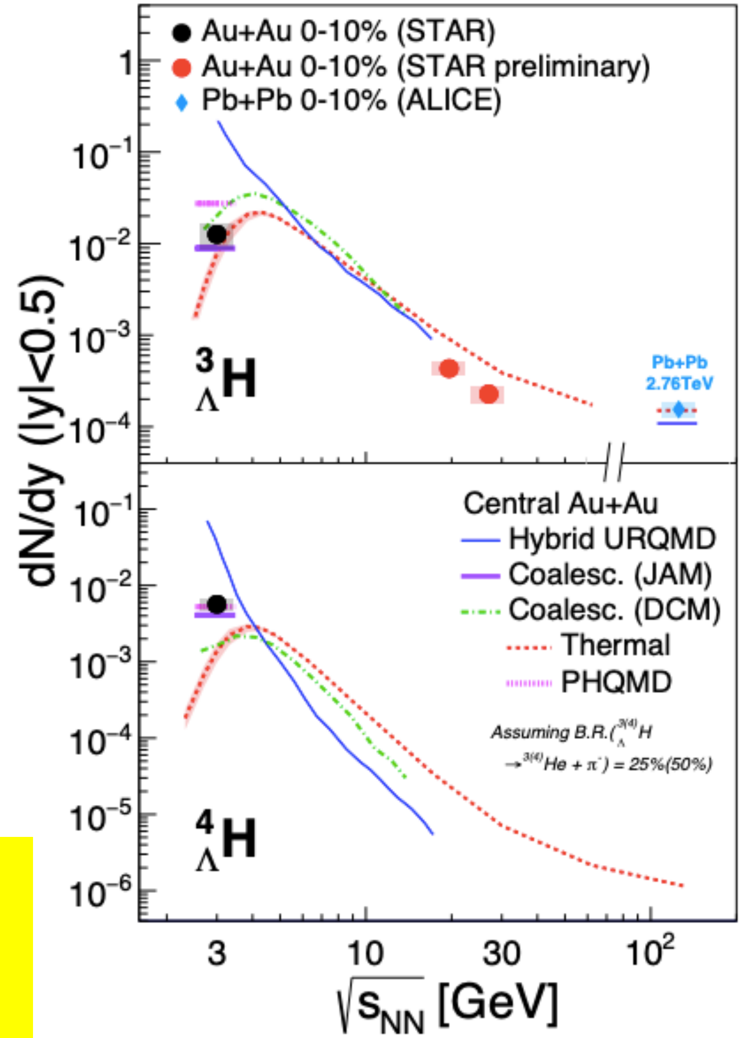

- First set of precision hypernuclei data from BES-II
- Towards quantitative understanding on ***Y-N*** interaction and high baryon density region

Energy Dependence of (Net-) Proton High Moments

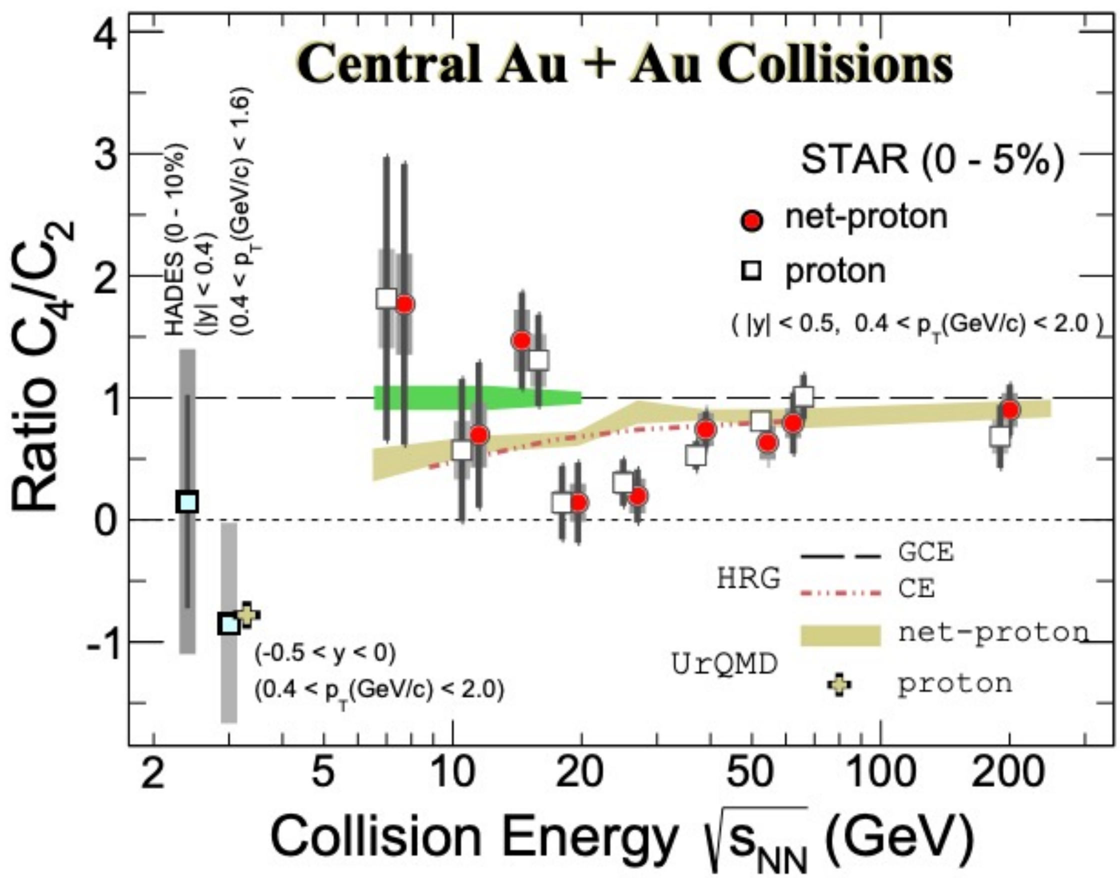

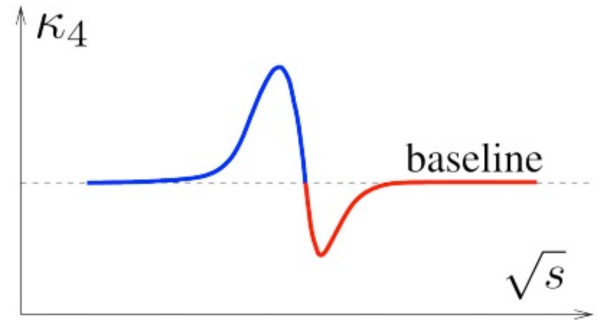

- Non-monotonic energy dependence in central Au+Au collisions (3.1σ)

- Strong suppression in proton C_4/C_2 at 3 GeV
  - consistent with UrQMD hadronic transport model calculation

BES-I: PRL 126 (2021) 092301
3 GeV data: PRL 128 (2022) 202303

Results at 3 GeV

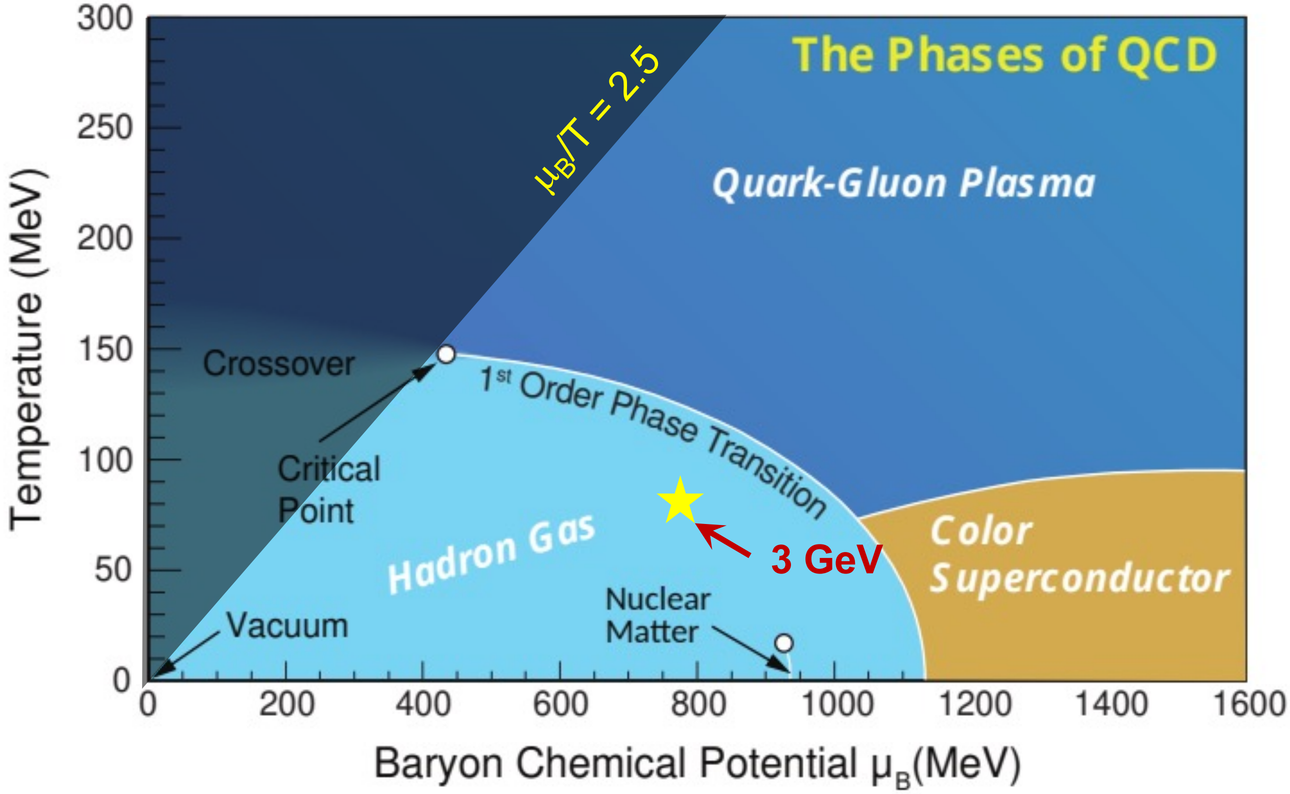

Lattice QCD predicts μ_B(CEP) > 400 MeV

BES-II

Au+Au collisions @ **3 GeV – hadronic phase**

- v_1/v_2 dominated by baryonic mean field
- ϕ/Ξ production driven by CE
- proton C_4/C_2 consistent with hadronic transport

Collective Flows from BES-II 19.6/14.6 GeV

- x2.5-4 reduction in v_1/v_2 statistical uncertainties @ 19.6 GeV

NCQ-scaling holds for particles (20%) while better for anti-particles @ 19.6 GeV

- transport quark effect

QM2022

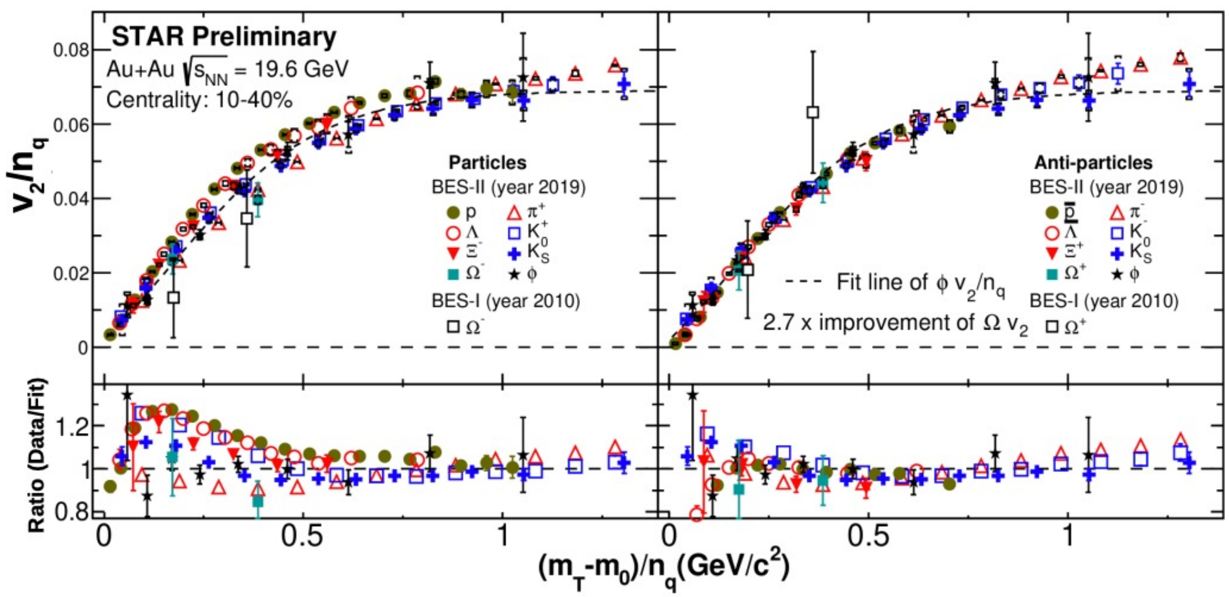

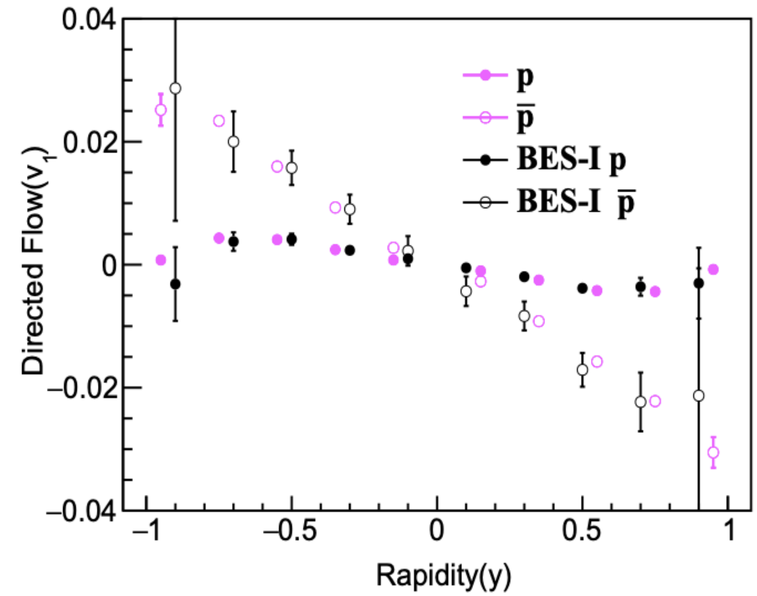

Status of BES-II Analyses

Year	Datasets	Calibration	Production	Analysis
2017/2018	54.4/27	Done	Done	Final
2018	FXT 3.0/7.2	Done	Done	Final
2019	19.6/14.6	Done	Done	Prel. @ QM22
	FXT	Done	Done	Post-prod QA
2020	11.5/9.2	in progress	Summer 2022	
	FXT	Done	Done	Post-prod QA
2021	7.7	in progress	Summer 2022	
	17.3	in progress	Fall 2022	
	FXT	in progress	Fall 2022	
	OO/dAu 200	*Fall 2022*		

Summary

Isobar (2018) and AuAu data

- Blinding analysis for CME search published
  - *Better baseline estimation and possible CME signal extraction under study*
- Many results on systematic measure of QGP medium properties and initial EM field

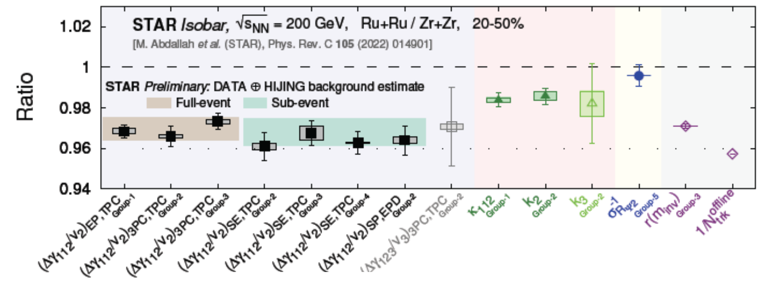

First set of BES-II results

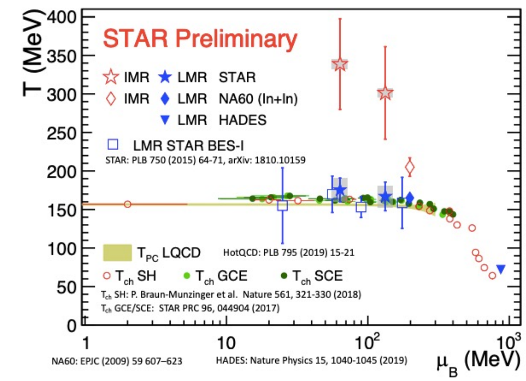

- FXT 3 GeV data (2018) demonstrate the dominance of hadronic phase
- Preliminary v_1/v_2 from 19.6/14.6 GeV: much improved precision compared to BES-I

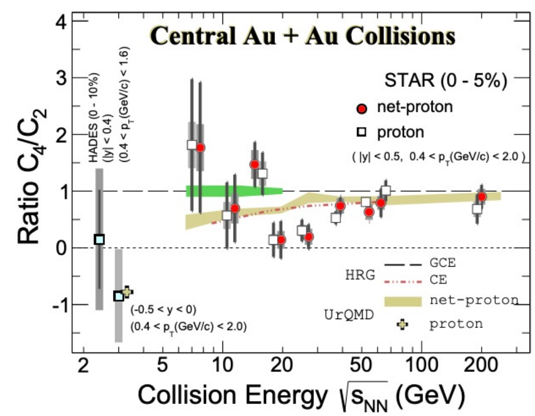

Results from full BES-II datasets to come out next year

- Backup

CME Analysis in Isobar Data

PRC 105 (2022) 014901

$$\kappa_{112} \equiv \frac{\Delta\gamma_{112}}{v_2\,\Delta\delta}$$

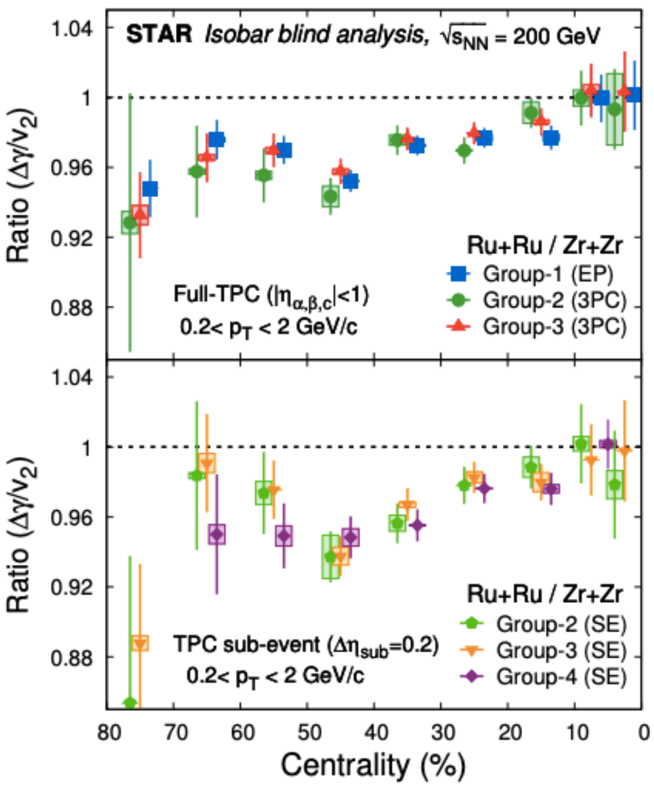

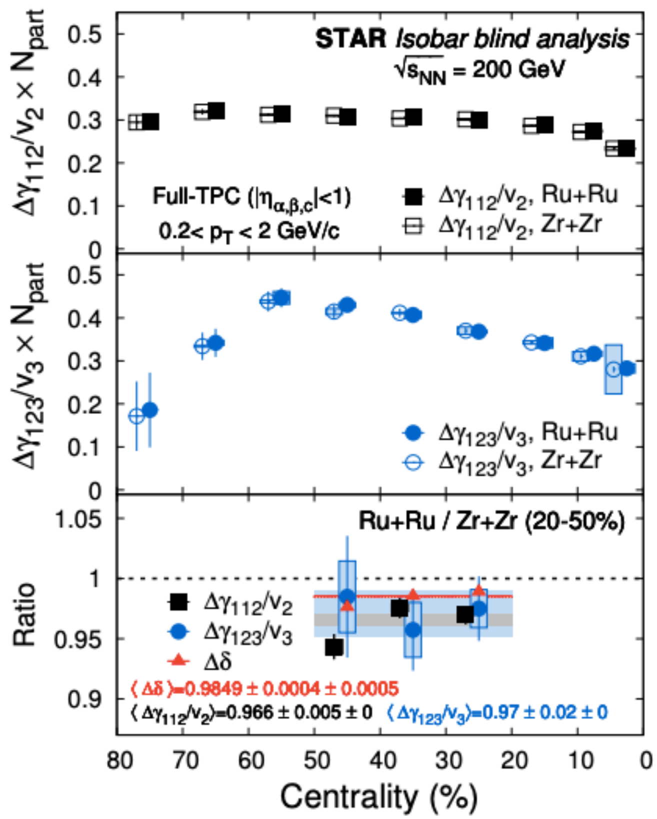

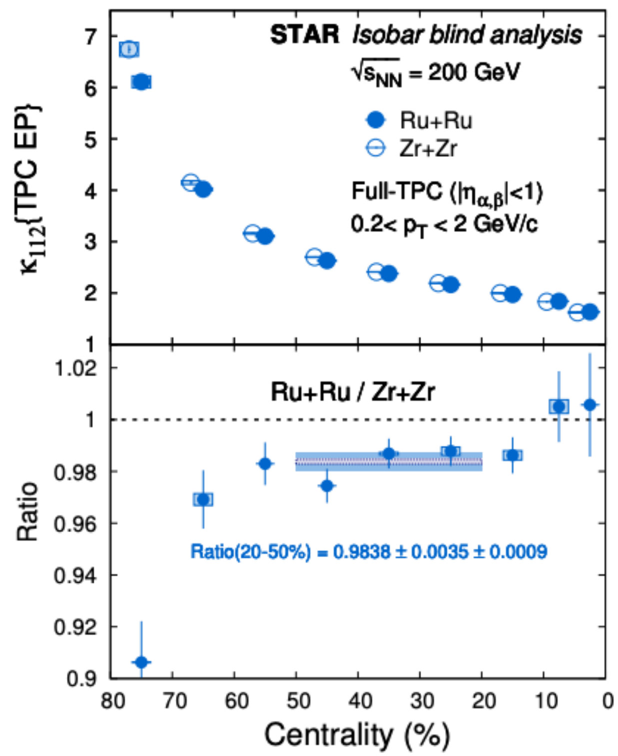

Consistency between different groups using the same method

Pre-defined CME signatures not observed:

$$\frac{(\Delta\gamma_{112}/v_2)^{\mathrm{Ru+Ru}}}{(\Delta\gamma_{112}/v_2)^{\mathrm{Zr+Zr}}} > \frac{(\Delta\gamma_{123}/v_3)^{\mathrm{Ru+Ru}}}{(\Delta\gamma_{123}/v_3)^{\mathrm{Zr+Zr}}} \qquad \frac{\kappa_{112}^{\mathrm{Ru+Ru}}}{\kappa_{112}^{\mathrm{Zr+Zr}}} > 1$$

New Estimate of Isobar Baseline for CME Signal

$$C_3 = \frac{C_{2\mathrm{p}} N_{2\mathrm{p}}}{N^2} v_{2,2\mathrm{p}} v_2 + \frac{C_{3\mathrm{p}} N_{3\mathrm{p}}}{2N^3} = \frac{v_2^2 \epsilon_2}{N} + \frac{\epsilon_3}{N^2}$$

$$\frac{N\Delta\gamma}{v_2^*} = \frac{NC_3}{v_2^{*2}} = \frac{\epsilon_2}{1+\epsilon_{\mathrm{nf}}} + \frac{\epsilon_3}{Nv_2^2(1+\epsilon_{\mathrm{nf}})} = \frac{\epsilon_2}{1+\epsilon_{\mathrm{nf}}}\left(1 + \frac{\epsilon_3/\epsilon_2}{Nv_2^2}\right)$$

$$\frac{(N\Delta\gamma/v_2^*)^{\mathrm{Ru}}}{(N\Delta\gamma/v_2^*)^{\mathrm{Zr}}} \equiv \frac{(NC_3/v_2^{*2})^{\mathrm{Ru}}}{(NC_3/v_2^{*2})^{\mathrm{Zr}}} \approx \frac{\epsilon_2^{\mathrm{Ru}}}{\epsilon_2^{\mathrm{Zr}}} \cdot \frac{(1+\epsilon_{\mathrm{nf}})^{\mathrm{Zr}}}{(1+\epsilon_{\mathrm{nf}})^{\mathrm{Ru}}} \cdot \frac{[1+\epsilon_3/\epsilon_2/(Nv_2^2)]^{\mathrm{Ru}}}{[1+\epsilon_3/\epsilon_2/(Nv_2^2)]^{\mathrm{Zr}}}$$

$$\approx 1 + \frac{\Delta\epsilon_2}{\epsilon_2} - \frac{\Delta\epsilon_{\mathrm{nf}}}{1+\epsilon_{\mathrm{nf}}} + \frac{\epsilon_3/\epsilon_2/(Nv_2^2)}{1+\epsilon_3/\epsilon_2/(Nv_2^2)}\left(\frac{\Delta\epsilon_3}{\epsilon_3} - \frac{\Delta\epsilon_2}{\epsilon_2} - \frac{\Delta N}{N} - \frac{\Delta v_2^2}{v_2^2}\right)$$

- v_2 nonflow and 2p nonflow are measured. 3p nonflow is estimated by HIJING. Large degree of cancellation between 2p and 3p nonflow.
- New preliminary isobar background estimate $\frac{(N\Delta\gamma/v_2^*)^{\mathrm{Ru}}}{(N\Delta\gamma/v_2^*)^{\mathrm{Zr}}} \approx (1.013 \pm 0.003 \pm 0.005)$ for full-event,
  $(1.011 \pm 0.005 \pm 0.005)$ for sub-event.
- ϵ_3 estimate in a data-driven way in future?

CME Search in Au+Au: PP vs. SP (ZDC)

$$f_{\rm CME} = \frac{\Delta\gamma_{\rm CME}\{\psi_{\rm PP}\}}{\Delta\gamma\{\psi_{\rm PP}\}} = \frac{A/a-1}{1/a^2-1}$$

$A = \Delta\gamma\{\psi_{\rm SP}\}/\Delta\gamma\{\psi_{\rm PP}\}$ $\quad a = v_2\{\psi_{\rm SP}\}/v_2\{\psi_{\rm PP}\}$

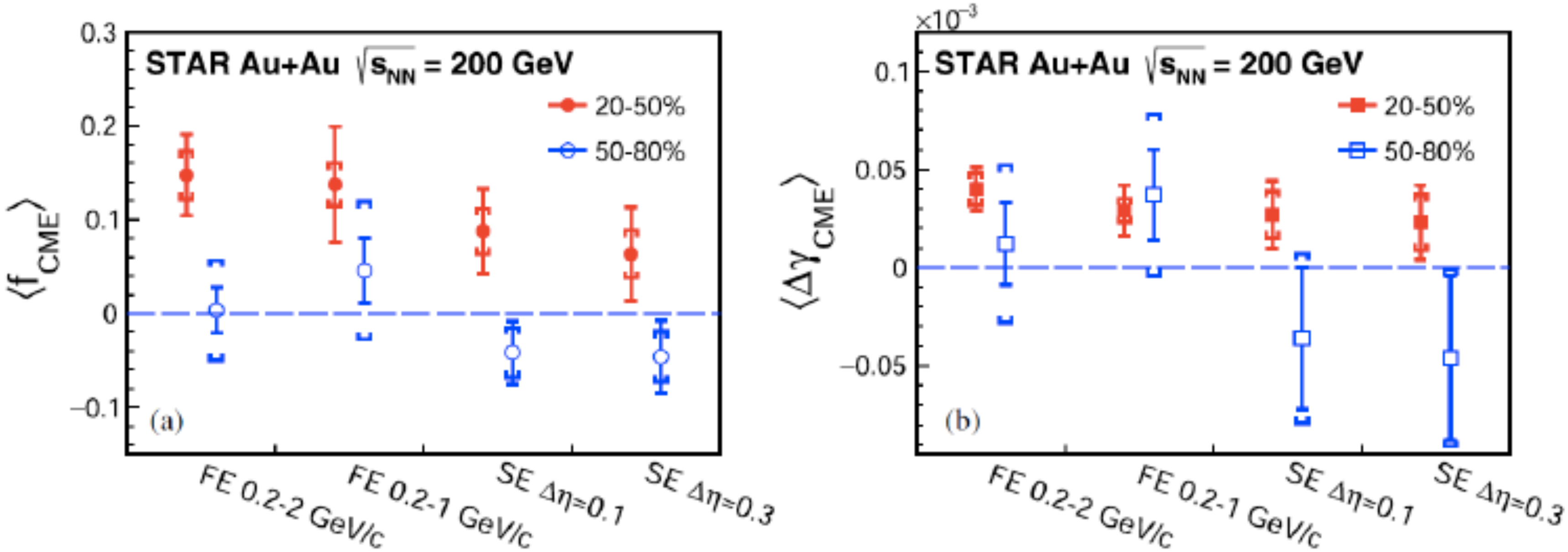

PRL 128 (2022) 092301

Hint of CME signal on the order of 1-3σ (2.4B Au+Au events)

CME S/B: isobar ~ 1/3 Au+Au *Y. Feng et al, PLB 820 (2021) 136549*

Initial EM Field on v_1 Splitting

Interplay between transported quarks and EM field

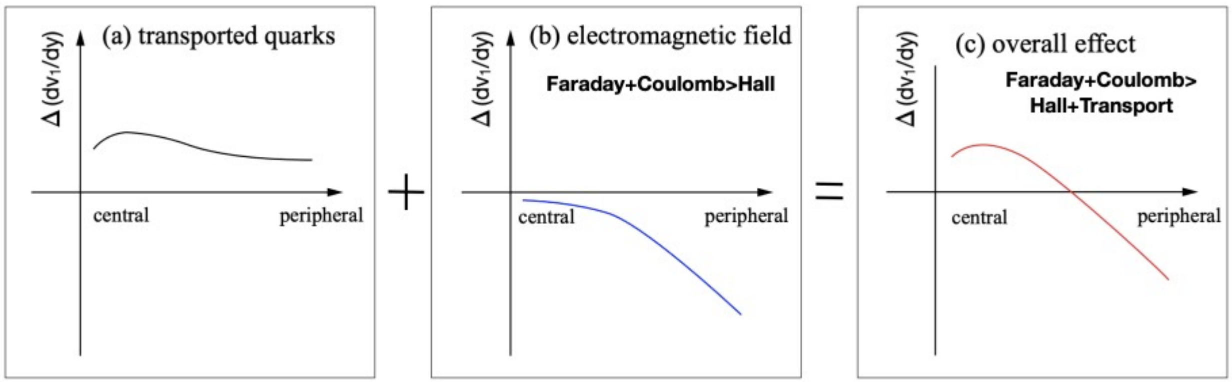

- Combinations having same or nearly same quark mass but different Δq and ΔS
  => No transported quark effect

Index	Quark Mass	Charge	Strangeness	Expression
1	$\Delta m = 0$	$\Delta q = 0$	$\Delta S = 0$	$[\bar{p}(\bar{u}\bar{u}\bar{d}) + \phi(s\bar{s})] - [K^{-}(\bar{u}s) + \bar{\Lambda}(\bar{u}\bar{d}\bar{s})]$
2	$\Delta m \approx 0$	$\Delta q = 1$	$\Delta S = 2$	$[\bar{\Lambda}(\bar{u}\bar{d}\bar{s})] - [\frac{1}{3}\Omega^{-}(sss) + \frac{2}{3}\bar{p}(\bar{u}\bar{u}\bar{d})]$
3	$\Delta m \approx 0$	$\Delta q = \frac{4}{3}$	$\Delta S = 2$	$[\bar{\Lambda}(\bar{u}\bar{d}\bar{s})] - [K^{-}(\bar{u}s) + \frac{1}{3}\bar{p}(\bar{u}\bar{u}\bar{d})]$
4	$\Delta m = 0$	$\Delta q = 2$	$\Delta S = 6$	$[\bar{\Omega}^{+}(\bar{s}\bar{s}\bar{s})] - [\Omega^{-}(sss)]$
5	$\Delta m \approx 0$	$\Delta q = \frac{7}{3}$	$\Delta S = 4$	$[\bar{\Xi}^{+}(\bar{d}\bar{s}\bar{s})] - [K^{-}(\bar{u}s) + \frac{1}{3}\Omega^{-}(sss)]$

A. Ikbal, D. Keane, P. Tribedy, Phys. Rev. C 105, 014912 (2022)

Azimuthal Dependence of ππ Photoproduction

c

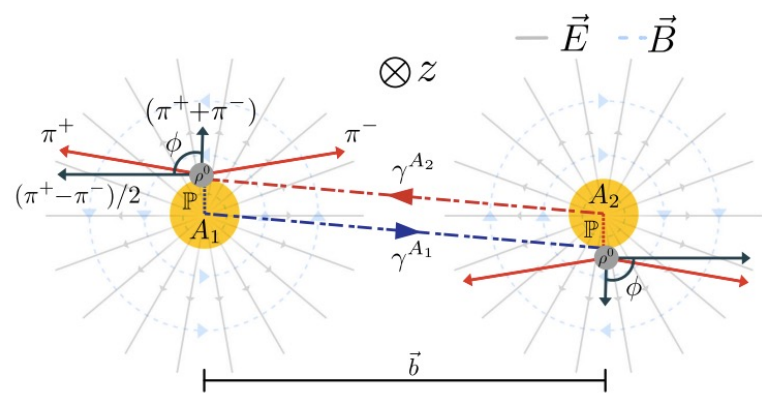

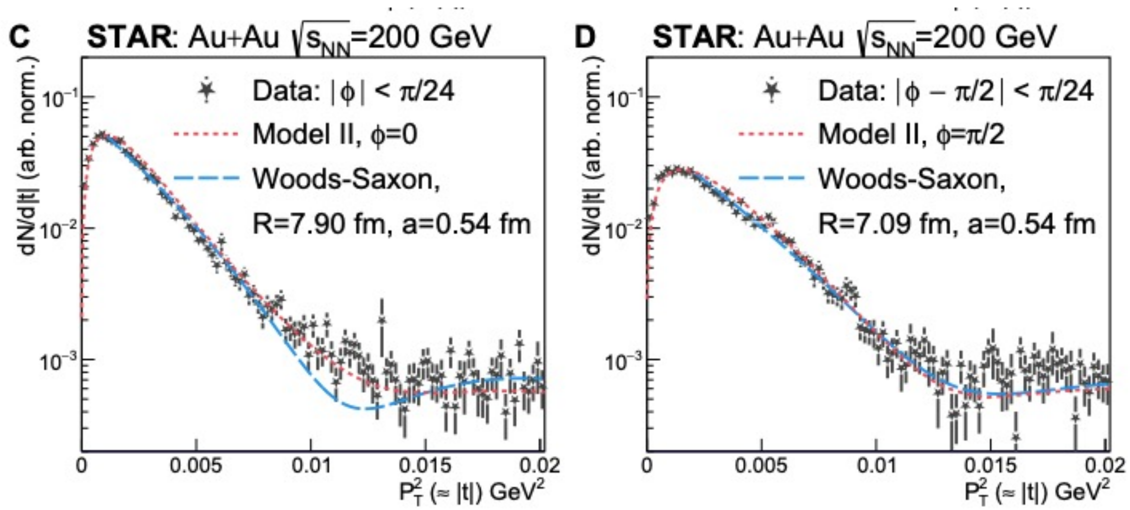

$$\cos\phi = (\vec{p_{T1}} + \vec{p_{T2}}) \cdot (\vec{p_{T1}} - \vec{p_{T2}})/(|\vec{p_{T1}} + \vec{p_{T2}}| \times |\vec{p_{T1}} - \vec{p_{T2}}|)$$

$$R = \sqrt{R_0^2 + \sigma_b^2/\epsilon_p \times (1 + \epsilon_p \cos 2\phi)}$$

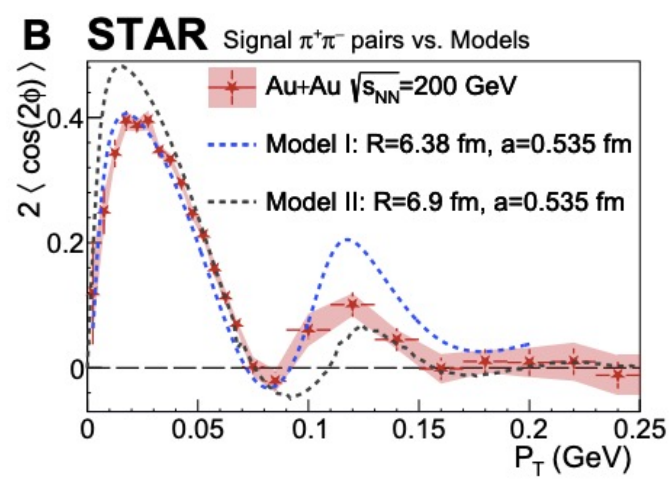

Local Polarization

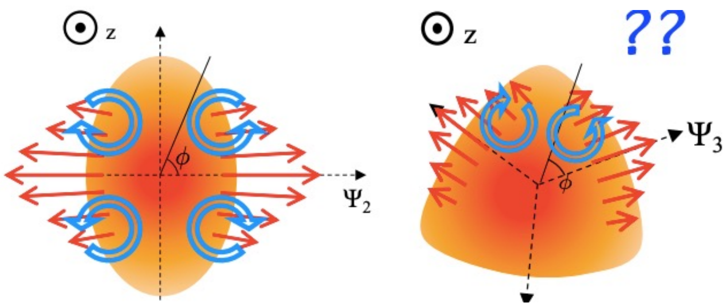

Longitudinal polarization due to anisotropic flows

First observation of v_3-driven polarization
New insight to thermal vorticity

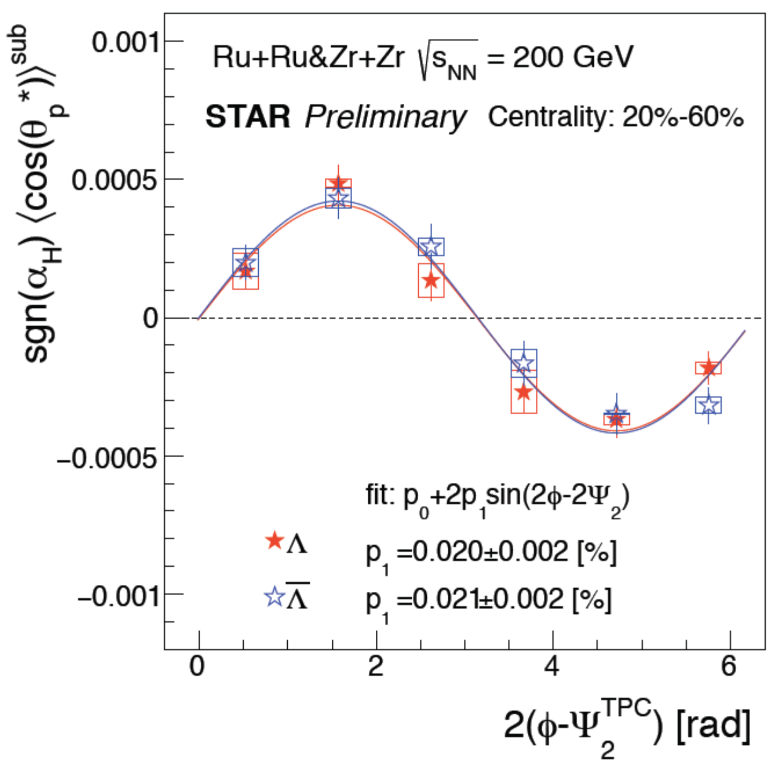

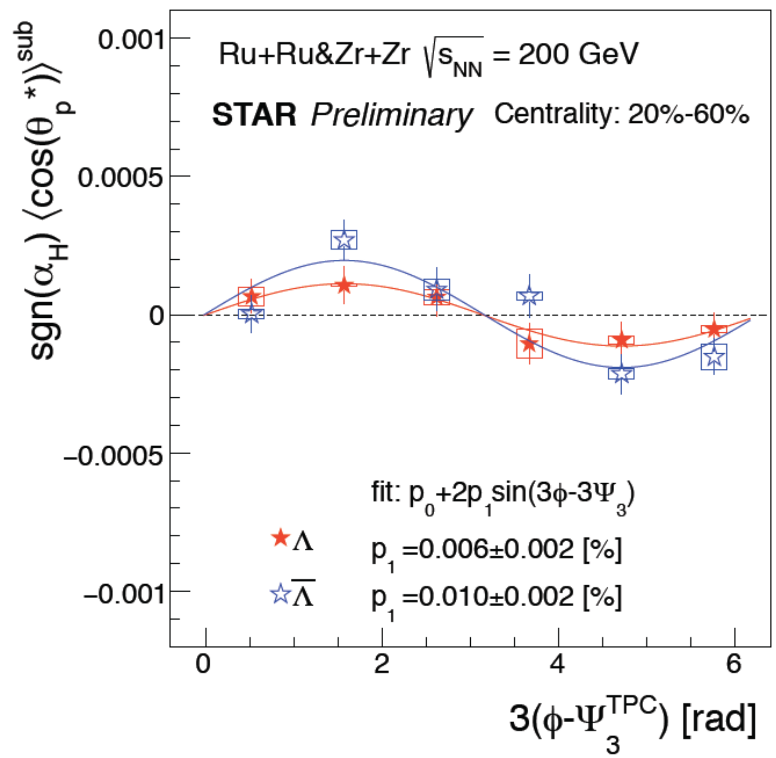

Heavy Flavor Jets

First measurement of D^0-tagged jets at RHIC using HFT

Suppression at low p_T for D^0-tagged jets
Ratio of *r*-dist. consistent with unity

→ New insights to heavy quark diffusion and energy loss in the QGP medium

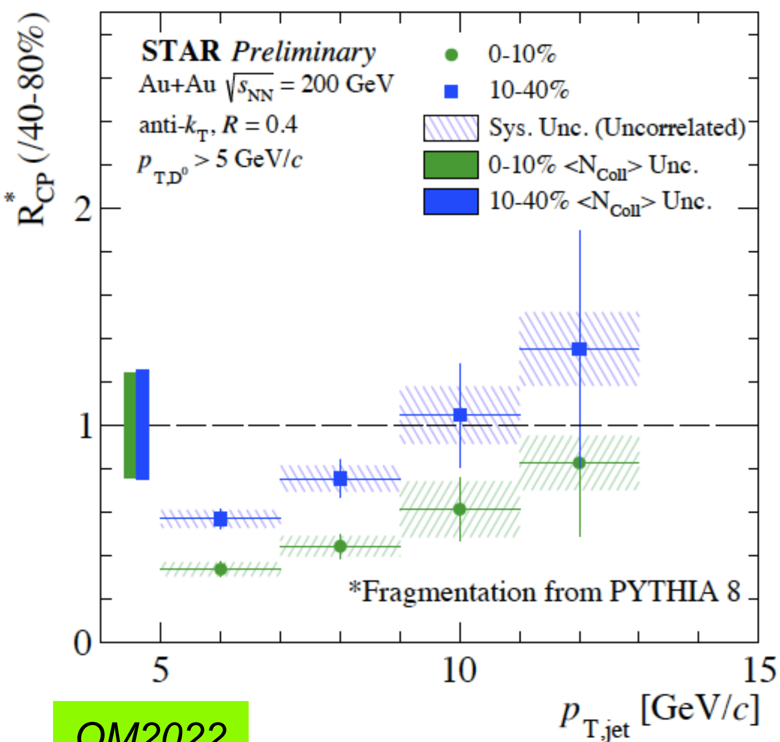

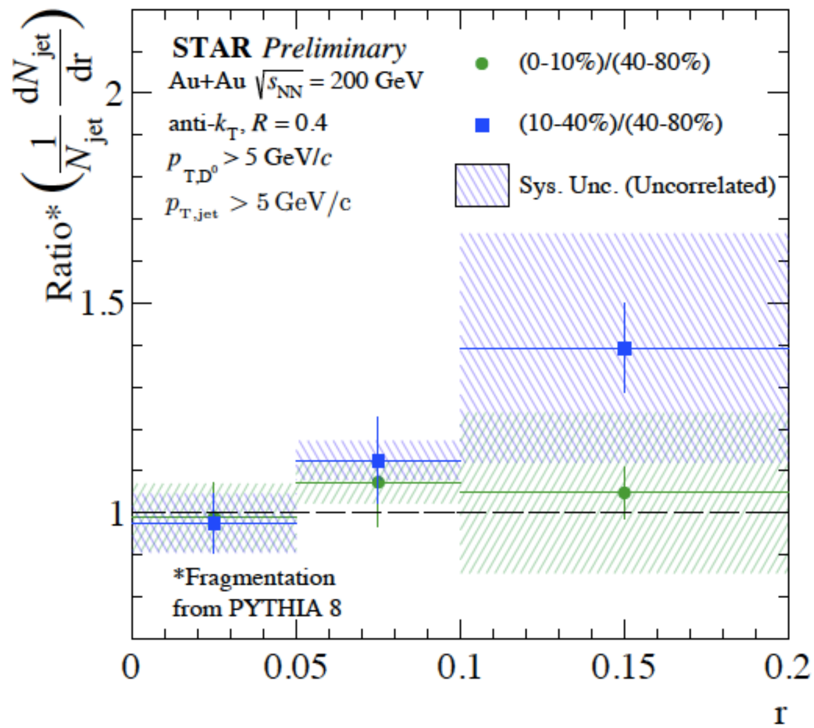

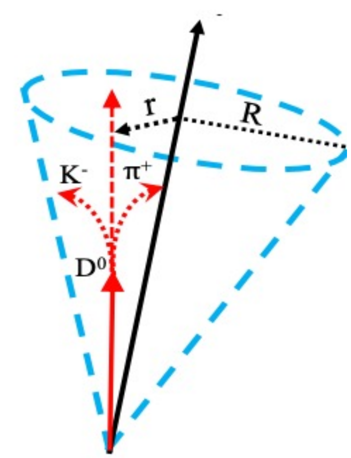

QM2022

Rapidity Window Scan of (Net-)Proton Fluctuations

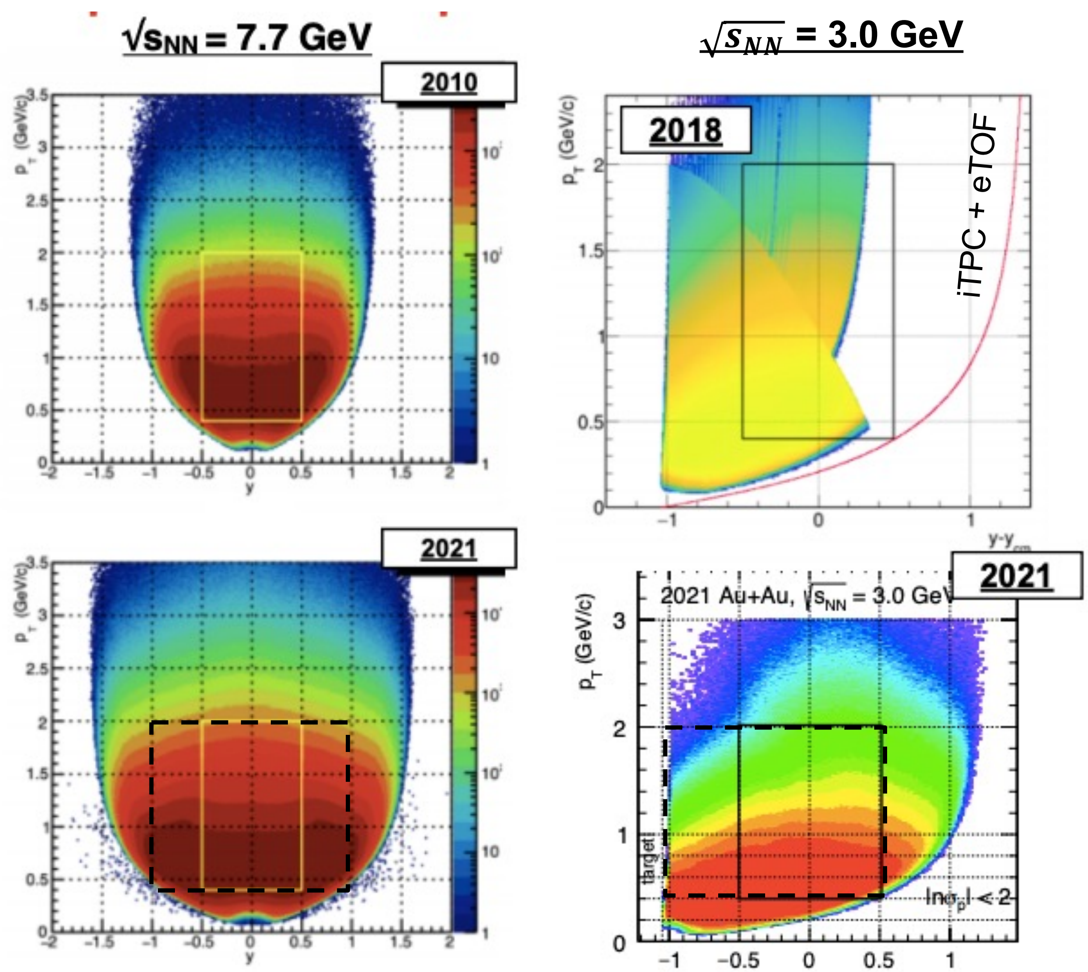

Rapidity windows at BES-II
Collider: |y|<0.8 (1.0)
FXT: -1.0<y<0.5 @ 3 GeV

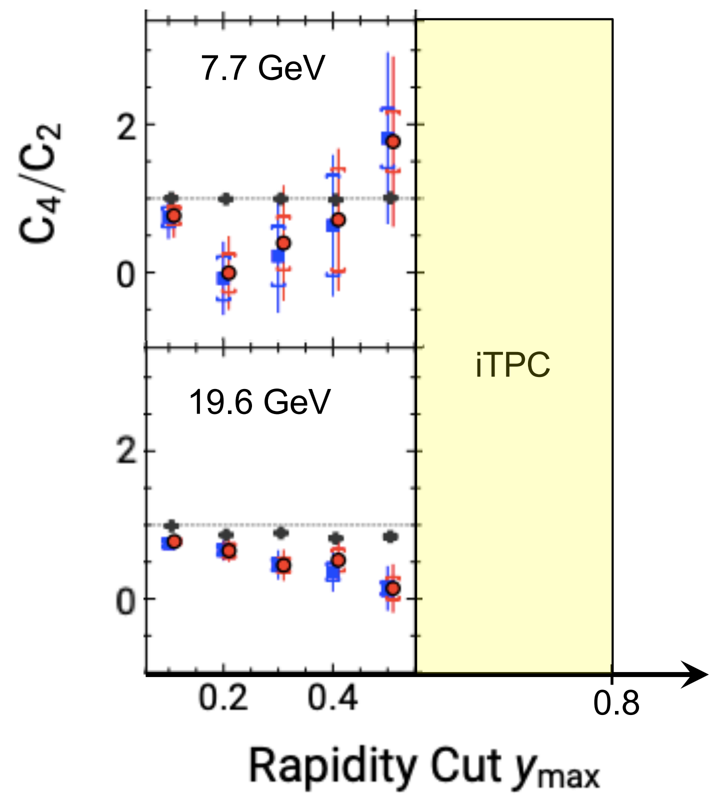

Full Coverage from y=0 to Target in 3 GeV Au+Au Collisions

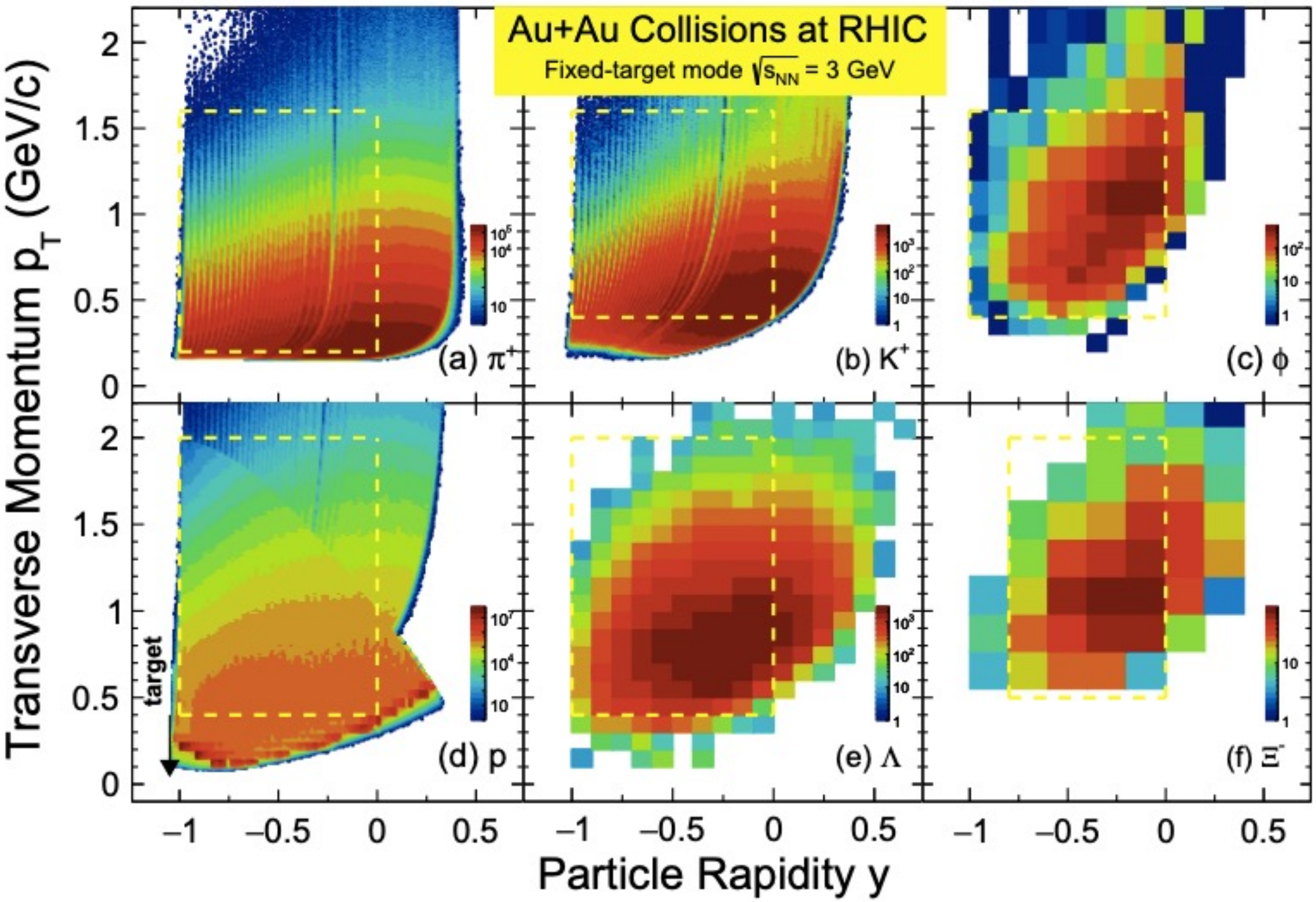

PLB 827 (2022) 137003

Directed/Elliptic Flows at 3 GeV

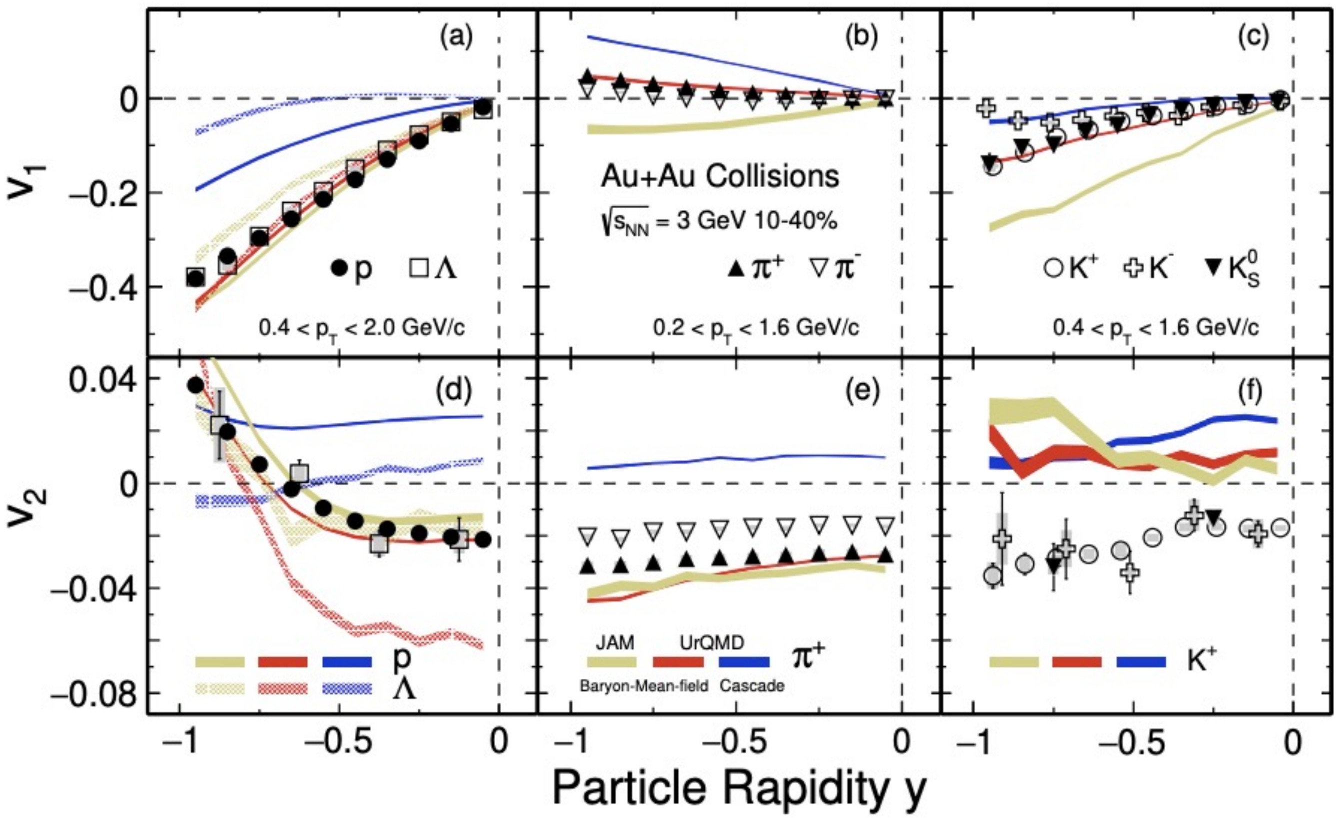

PLB 827 (2022) 137003

- Midrapidity v_1 slope positive for all particles (negative at high energies)
- Midrapidity v_2 negative for all particles (positive at high energies)

  - UrQMD/JAM with baryonic mean field describe proton v_1/v_2 data

(Net-)Proton Directed Flow

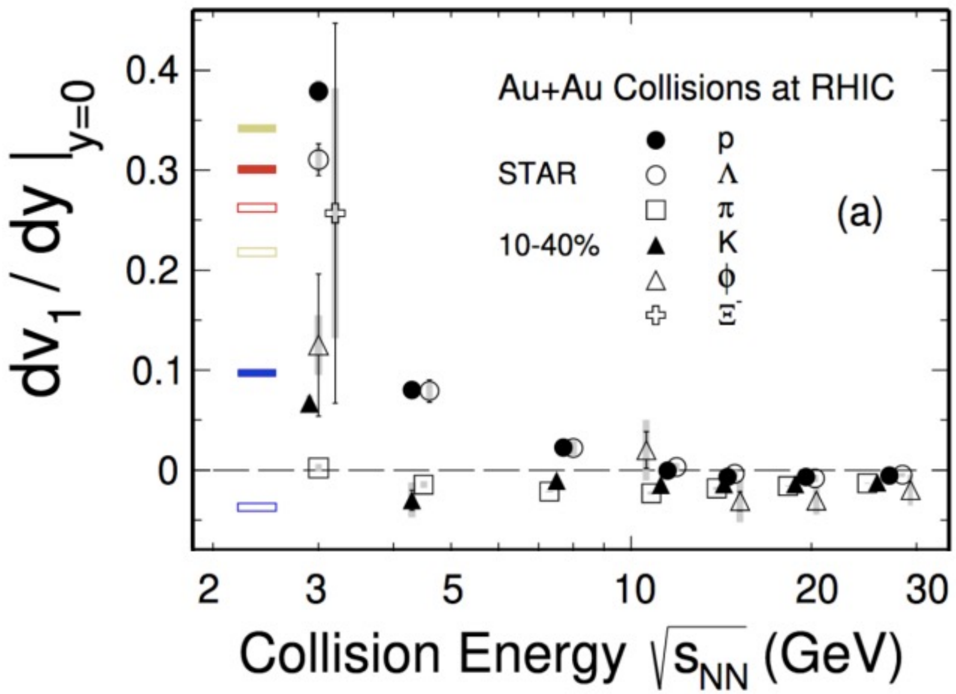

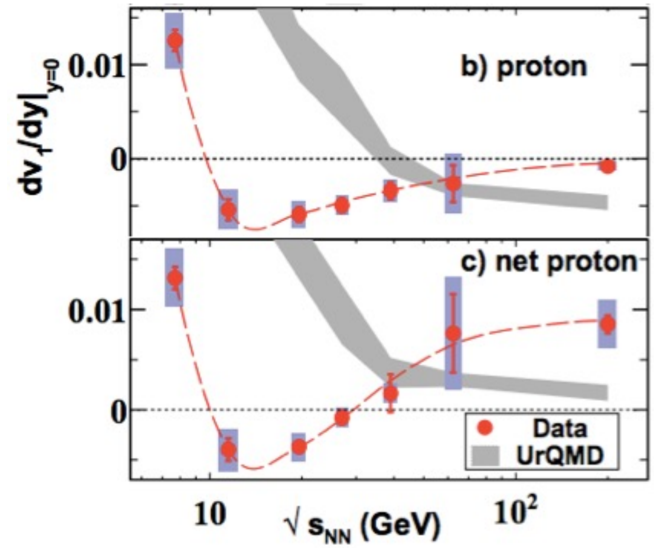

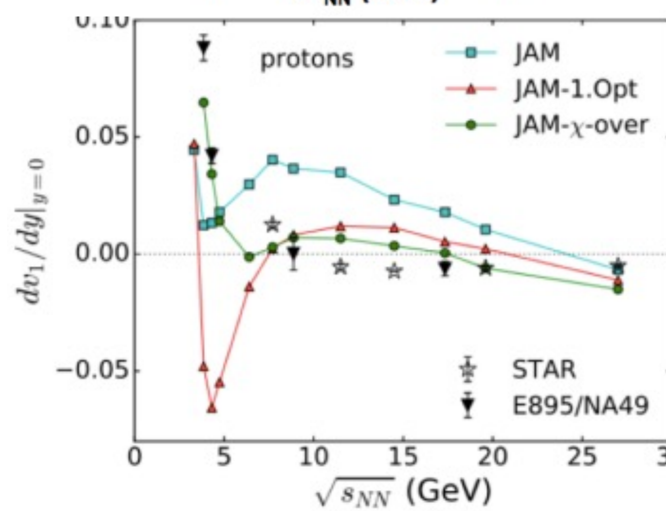

Y. Nara et al, PLB 769 (2017) 543

- Nearly all particle v_1 slopes are positive at 3 GeV
- Proton/net-proton v_1 vs. energy show a minimum
  - *- Connection to 1st order phase transition?*
  - *- model predicts a dip at much lower energy*

BES-II Prospects: Statistics and Systematics

Significantly improved statistics and systematics

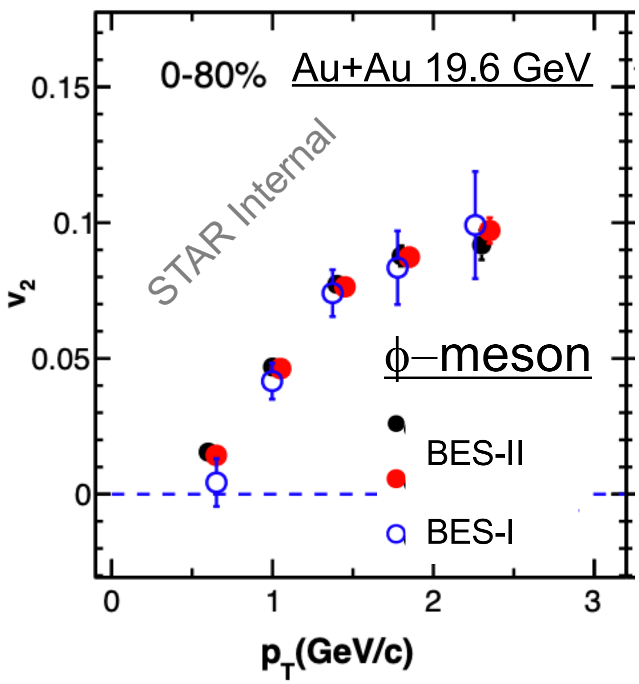

TPC Tracking Efficiency Uncertainty

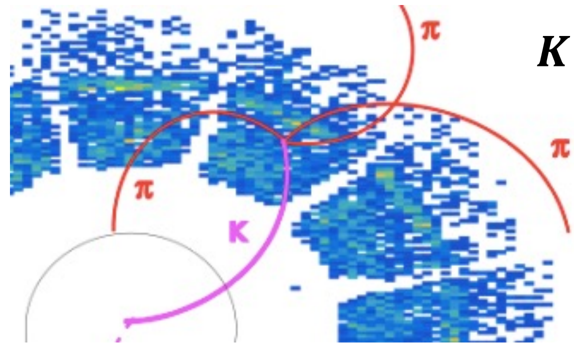

$K \rightarrow \pi\pi\pi$

$$\varepsilon = \frac{K_{Vtx}(3\pi) + K_{rc}}{K_{Vtx}(3\pi)}$$

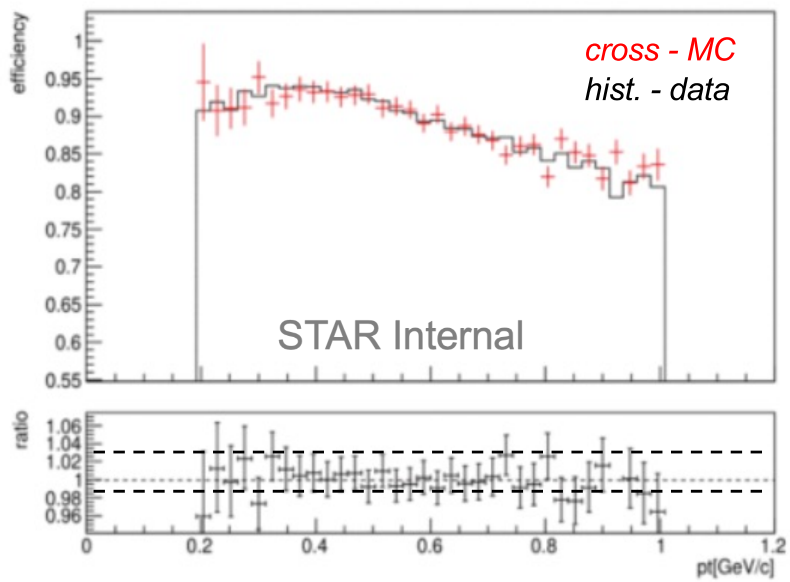

σ_{eff} **< 2%**